TURBOMACHINERY & PUMP SYMPOSIA | HOUSTON, TX
DECEMBER 14-16, 2021
SHORT COURSES: DECEMBER 13, 2021

A PRACTICAL GUIDE TO UNDERSTANDING LATERAL ROTORDYNAMIC ANALYSIS TO HELP IDENTIFY AND SOLVE VIBRATION PROBLEMS IN TURBOMACHINERY

Patrick J. Smith
Air Products Fellow
Air Products & Chemicals
Allentown, PA, 18195 USA

John Whalen
Consultant
Houston, TX 77062, USA

Dustin Pavelek, P.E.
Senior Consulting Engineer
Kelm Engineering
Houston, TX 77059 USA

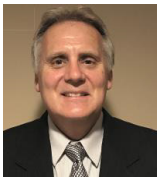

Patrick Smith is an Air Products Fellow in the Operation Excellence Technical Team at Air Products & Chemicals. He is based in Allentown, PA, and he is the Machinery Technology Manager and the Machinery Functional Lead for Global Operations. As Machinery Technology Manager he provides a balanced approach to the assessment and mitigation of technical risk for rotating machinery. As Machinery Functional Lead for Global Operations he provides solutions for difficult rotating machinery problems that have broad applications or have a significant impact on safety, reliability, or performance. Patrick started his career with Ingersoll-Rand in the Pump Division in 1982 after graduating from Villanova University with a B.S. Degree in Mechanical Engineering. He joined Air Products & Chemicals, Inc. in 1986 working as a rotating machinery specialist. He went on to get a Masters in Mechanical Engineering from Villanova University in 1990. He has published dozens of articles on rotating machinery. He is also a registered professional engineer in the state of Pennsylvania and has been a member of the Turbomachinery Advisory Committee since 2016.

John Whalen spent seven years (1981-1987) at Dresser-Rand Steam Turbines as a Product Engineer in the Large Turbine Engineering Department and then as an Analytical Engineer in the Rotordynamics Group of the Advanced Engineering and Development Department. In 1988, John accepted a position with Centritech Corporation, as the Assistant Chief Engineer. In 1989, he was promoted to Manager of Engineering. In 1991, he left Centritech to help start TCE/Turbo Components & Engineering, Inc. At TCE, he was responsible for the Engineering Department and engineering for the product lines, which include babbitted journal and thrust bearings, labyrinth seals and related engineering services. John was president and primary owner of TCE when it was acquired by John Crane in 2011, John retired from John Crane in 2015. In August of 2018 John agreed to support Gulf Coast Bearing & Seal (GCBS) in a consulting role as their Chief Engineer. John received his BSME (1981) from Rochester Institute of Technology. John is a registered Professional Engineer in the State of Texas and holds an Emeritus position on the Turbomachinery Symposium Advisory Committee.

Dustin Pavelek is a Sr. Consultant with Kelm Engineering, LLC where he is responsible for conducting analytical studies and field vibration testing for rotating and reciprocating machinery. He previously served as a member of corporate Machinery Engineering and PdM groups in the petrochemical and power generation industries. He is a proud graduate of Texas A&M University and holds a B.S. and an M.S. in Mechanical Engineering. Pavelek is a registered professional engineer in the States of Texas and Louisiana and is a Certified ISO Category IV Vibration Analyst through the Vibration Institute.

ABSTRACT

The primary purpose of performing a lateral rotordynamic analysis for centrifugal compressors, steam turbines and other rotating machines is to ensure that there are no undesirable rotor/bearing performance issues that result in high or unstable rotor vibrations. This is accomplished by predicting lateral critical speeds, evaluating response due to unbalance, and evaluating if there are any self-excited vibrations that could result in unstable vibration. In doing so manufacturers use rotordynamics to design the shafting,

bearings, seals, etc., as well as establishing criteria for component weights (such as impellers, sleeves, couplings, etc.) and component fits. API standards, such as API-617, define the analyses to be done and the acceptance criteria. Understanding this aids in rotor balancing and helps ensure successful shop tests and field commissioning.

However, things do not always go as planned. What happens when actual rotordynamic behavior is different than predicted behavior? What happens if vibration behavior changes over time? Knowing how to interpret rotordynamic analyses can help end users identify potential issues on new machines as well as help with troubleshooting if the vibration behavior changes over time. This tutorial will touch on some of the theory of lateral rotordynamics at a high level, but the purpose of this tutorial is to help end users understand lateral rotordynamic reports, ensure that nothing is missed in the analysis, and demonstrate how this information can be used to help identify and solve vibration problems in turbomachinery.

INTRODUCTION

This tutorial will primarily focus on lateral rotordynamics of inline and integrally geared centrifugal compressors, although the basic principles apply to any rotating machine. And one of the case studies involves a motor that is driving a compressor. The body of the tutorial is divided into the following five sections.

- Basic theory
- Key elements of a rotordynamic analysis
- Understand and interpret a rotordynamic analysis
- Examples of deficiencies in reports that changes the analysis
- Case studies showing how an understanding of rotordynamics helped identify and solve a vibration problem

The tutorial begins with a simple spring and mass model that will be used illustrate the basic concepts of a vibrating mechanical system. This simple single degree of freedom model will cover free (undamped) vibration, free vibration with damping, and damped forced vibrations. This model will then be extended to simple rotor supported by bearings to provide an example calculation of undamped natural frequency, damped natural frequency, magnification factor, logarithmic decrement (log dec) and amplitude of vibration. This will then be discussed in the next section to explain the key elements of a rotordynamic analysis.

Building on this, the next section will explain how to understand and interpret a rotordynamic analysis report for a centrifugal compressor rotor. This will help end users evaluate a rotordynamic analysis to ensure it is complete, all conditions are analyzed and that the results meet the acceptance criteria. Understanding a rotordynamic report can also be a useful when troubleshooting a vibration problem on the test stand or in the field.

There are different industry and company standards that cover acceptance criteria for a lateral rotordynamic analysis. API-617 is commonly used for axial and centrifugal compressors and expanders. However, it is not enough just to verify that the analysis meets API-617 criteria. There can be critical cases and conditions that need to be considered that could change the outcome of the analysis. So, understanding rotordynamics can also be used to evaluate if there are deficiencies in the reports which can change the analysis. Examples of this will be presented in this tutorial.

Finally, five case studies will be presented to show how understanding a rotordynamic analysis was useful in preventing or solving a vibration problem.

BASIC THEORY

Vibration is defined as oscillatory motion about an equilibrium point. Vibration can be characterized as either free or forced. Free vibration occurs when a disturbing force is applied once and then removed. An example of this would be hitting a tuning fork. In this case the tuning fork will vibrate at its free or natural frequency. Forced vibration occurs when a time varying disturbing force is applied to a mechanical system. This force can be harmonic (occurring at the same frequency) or non-harmonic. Unbalance in a rotating shaft is an example of a harmonic disturbing force. Vibration of a car on a rough road is an example of a non-harmonic disturbing force.

Let's start the discussion with free vibration. An example of a simple single degree of freedom mechanical system is a mass hanging from a spring that is displaced and released as shown in Figure 1. In this case the mass oscillates up and down as shown in Figure 2.

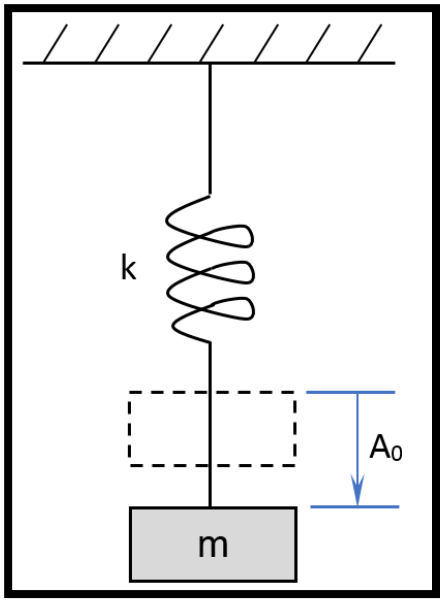

Figure 1: Mass Hanging from a Spring and Displaced

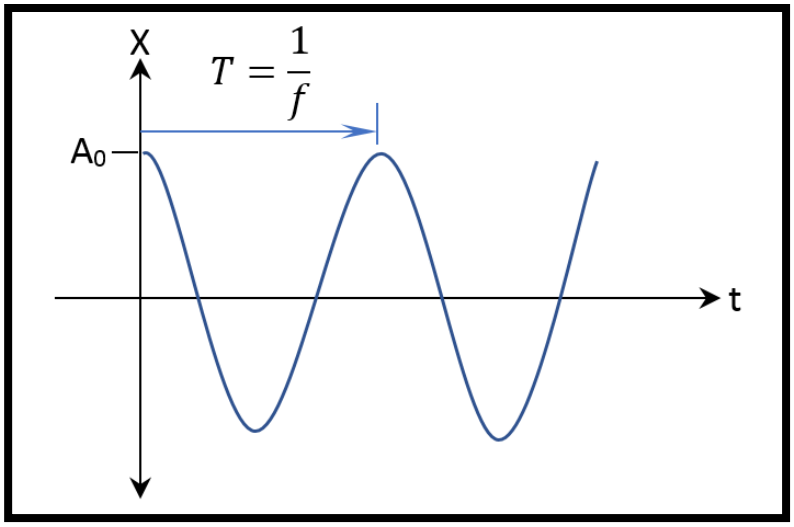

Figure 2: Motion of Spring

Neglecting friction in this simple system, the equation of motion is:

$$\Sigma F = 0;\ -ma - kx = 0; m\frac{d^2x}{dt} = -kx \tag{1}$$

Where:
F = Force
m = Mass
a = Acceleration
k = Spring stiffness
x = Displacement
t = Time

Solving this equation leads to the following result:

$$\omega = \sqrt{\frac{k}{m}} \tag{2}$$

Where
ω = Undamped natural frequency

Without friction, this motion would continue indefinitely. What this says is that the natural frequency is a function of stiffness and mass. As we expand this simple system to more complex mechanical systems, this simple formula can be used to understand the system behavior and how it changes when stiffness or mass are changed. For example, increasing stiffness raises the natural frequency and increasing mass lowers it . This is probably the most important formula to remember when evaluating rotordynamic behavior.

Vibration can also be characterized as damped or undamped. Damping is a reduction in the amplitude of oscillation due to friction or some other resistance force. If there is no damping, the mass shown in Figure 1 will oscillate up and down indefinitely. If there is damping, the oscillation will decay with time. All systems have some damping. Even a solid steel ball bearing for example has some damping, although not very much. Fluid film or magnetic bearings could have quite a lot. Damping removes energy from the vibration by turning it into heat. This requires movement and the amount of damping is a function of velocity. Getting back to the example of the mass hanging by a spring under free vibration, damping can be represented as a dashpot as shown in Figure 3:

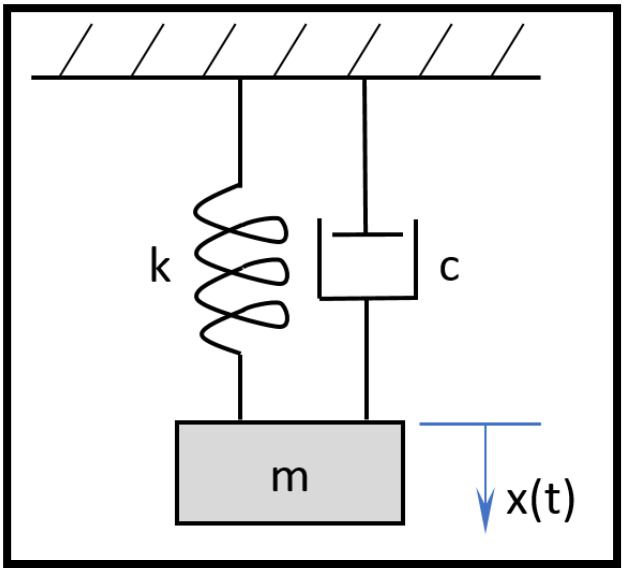

Figure 3: Mass Hanging By A Spring with Damping

The viscous damping force can be represented by the following formula:

$$F = Cv = C\frac{dx}{dt} \tag{3}$$

Where:
C = Coefficient of viscous damping
υ = Velocity

Putting this altogether, the equation of motion for this simple spring system is:

$$m\frac{d^2x}{dt} + C\frac{dx}{dt} + kx = 0 \tag{4}$$

Solving this equation leads to the following result:

$$\omega_d = \sqrt{\frac{k}{m} - \left(\frac{C}{2m}\right)^2} \tag{5}$$

Where:
ω_d = Damped natural frequency

If the natural frequency is zero, the mechanical system doesn't vibrate when a disturbing force is applied. It acts like a rigid body and the system deflects and then returns to its original position after the force is applied without oscillating. In this case the system is said to be "critically damped." Said another way, critical damping is the minimum amount of viscous damping that results in a displaced system returning to its original position without oscillation. Looking at equation (5), the critical damping coefficient would be:

$$C_{Crit} = 2\sqrt{mk} \tag{6}$$

Where:
C_{crit} = Critical damping coefficient

The damping ratio is the damping coefficient C divided by critical damping coefficient

$$\zeta = \frac{C}{C_{crit}} \tag{7}$$

Where:
ζ = Damping ratio

Critical damping is the threshold between a mechanical system that is overdamped versus one that is underdamped. A system that is overdamped, ($\zeta > 1$) will gradually return to equilibrium but will not oscillate after a disturbing force is applied. An automatic door close is an example of an overdamped system. A system that is lightly damped ($\zeta < 1$) will oscillate with diminishing amplitude after a disturbing force is applied. A diving board with a diver is an example of an underdamped system. The diving board deflects when the diver dives, and then the board oscillates up and down until it returns to its original position.

If we re-arrange equations (5) and (7), the damped natural frequency as a function of the critical damping ratio is:

$$\omega_d = \omega\sqrt{1 - \zeta^2} \tag{8}$$

A term that is commonly used to evaluate the stability of a mechanical system is the log dec, which is defined as the natural logarithm of the ratio of two successive amplitudes and is calculated from the following formula.

$$\delta = \frac{2\pi\zeta}{\sqrt{1-\zeta^2}} \tag{10}$$

Where:
δ = Log dec

A positive log dec indicates that the system is stable and the vibration decays with time. A log dec of zero indicates that the vibration neither decays nor grows with time. And a negative log dec indicates that the vibration amplitude grows with time. See Figure 4.

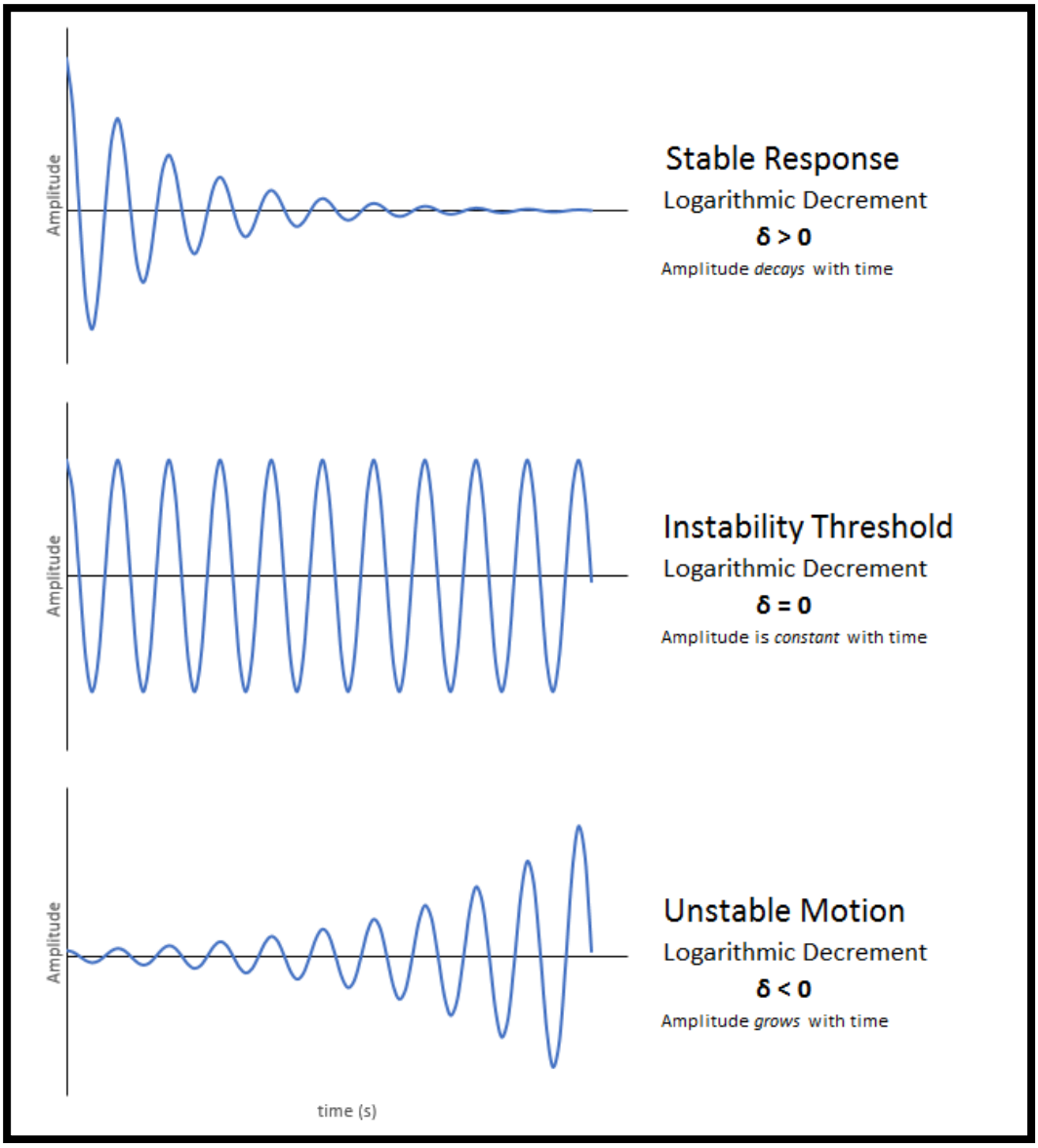

Figure 4: Amplitude Behavior as a Function or Log Dec

Now, what happen if there is a time varying disturbing force is applied to this simple mechanical system. This is an example of damped forced vibrations. See Figure 5.

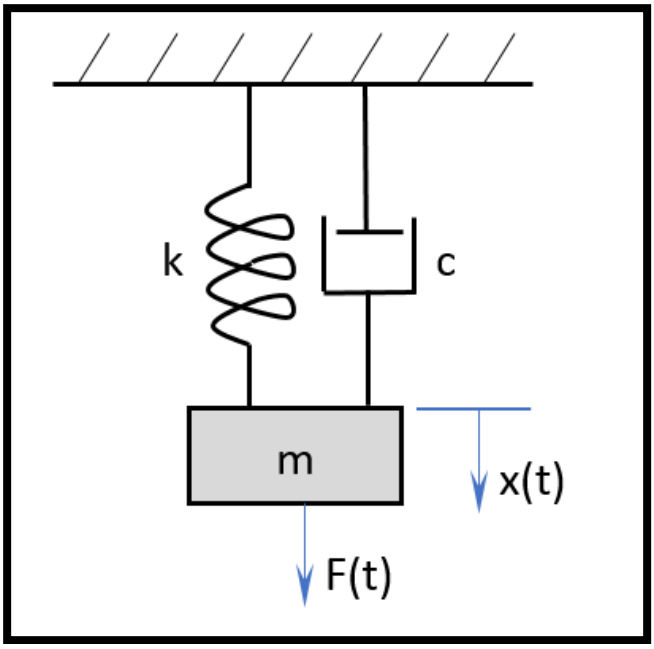

Figure 5: Damped Forced Vibrations

The equation of motion for this system is:

$$m\frac{d^2x}{dt} + C\frac{dx}{dt} + kx = F(t) \tag{11}$$

The solution to this equation has several terms, one of which is equation (12), the damped magnification factor for steady state forced vibrations.

$$\beta_d = \left| \frac{1}{\sqrt{\left(1-\left(\frac{\omega_f}{\omega}\right)^2\right)^2 + \left(\frac{C\omega_f}{\omega\sqrt{km}}\right)^2}} \right| \tag{12}$$

Where:
β_d = Damped magnification factor
ω_f = Forcing function frequency

The undamped magnification factor would not include the second term in the denominator in equation (12) since the damping coefficient, C, would be zero. And, in this case, if the forcing function frequency is the same as the natural frequency, the denominator would be zero and the magnification factor would be infinity. But there always is some damping and if there is sufficient damping, the damped magnification factor can be very small. A good way to illustrate this is shown in Figure 6. This is a plot of the rotor speed (frequency) divided by the natural frequency versus the amplitude magnification for various damping ratio values.

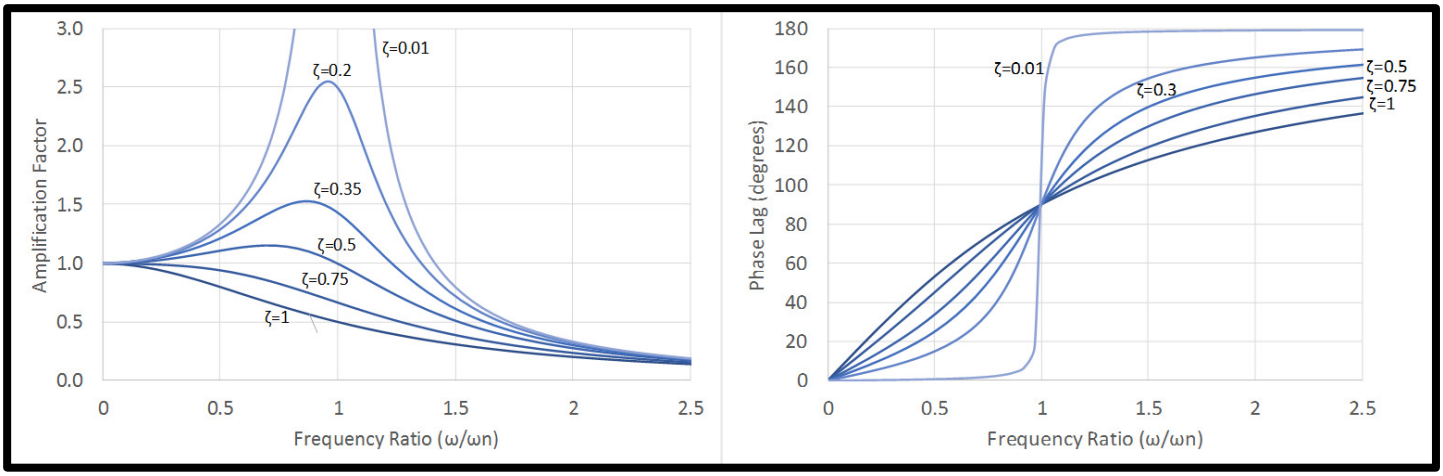

Figure 6: Amplification Factor and Phase Lag vs. Frequency Ratio

Up to this point we've looked at a simple mass supported by a spring. But this same approach can be used for rotating shafts. A shaft's natural frequency is referred to as the critical speed. This is the rotational speed that equals the lateral natural frequency of vibration. It is really just an extension of lateral vibration (moving up and down) vibration in beams. Let's look at a simple example.

PROBLEM: Rotor with a single disc mounted between bearings. See Figure 7.

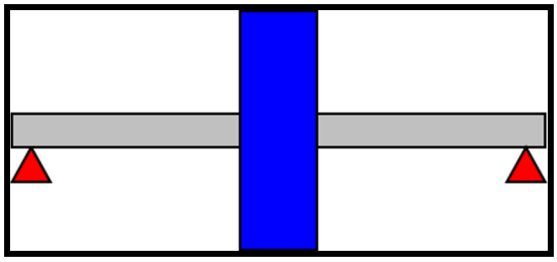

Figure 7: Single Disc Between Bearings

GIVEN:

- Weight of Disc = 2200 N
- Neglect mass of shaft for this example
- Speed = 1000 RPM
- Unbalance = 88 gm-m
- K_{shaft} = 8,750 N/mm
- k_{brg} = 21,900 N/mm
- C_{brg} = 4.4 N-sec/mm

FIND:

- Undamped natural frequency
- Damped natural frequency
- Magnification factor
- Log dec
- Amplitude of vibration

Since each bearing has the same stiffness and damping, this rotor bearing system can be modeled as a simple spring mass damper system as shown in Figure 5. The effective stiffness can be calculated from the following equation.

$$k_{eq} = \frac{2}{\frac{2}{k_{shaft}} + \frac{1}{k_{brg}}} \tag{13}$$

The equivalent stiffness works out to 7293 N/mm. The equivalent damping is determined in a similar manner and works out to 8.8 N-sec/mm. The mass works out to 224 kg.

- Using equation (2), the undamped natural frequency works out to: $\omega = 28.7$ Hz = 1722 CPM
- Using equations (6) and (7), the damping ratio works out to: $\zeta = 0.109$
- Using equation (8), the damped natural frequency works out to: $\omega_d = 28.53$ Hz = 1712 CPM
- Using equation (10), the log dec works out to: $\delta = 0.688$
- Using equation (12), the damped magnification factor at the operating speed works out to: $\beta_d = 1.482$

Unbalance creates a disturbing force that occurs at a frequency equivalent to the running speed 16.7 Hz (1000 RPM), or an angular forcing frequency of 104.7 radians/second. The out of balance force can be determined by multiplying the unbalance by the square of the angular forcing frequency. This works out to 965 Newtons. The amplitude of vibration can be determined by multiplying the magnification factor by the unbalance force divided by the equivalent stiffness. This works out to 0.2 mm.

Although this simple problem doesn't reflect a real rotordynamic analysis of a turbomachine, it follows a similar method. A real turbomachine is more complex and there are different tools to more accurately predict a rotordynamic behavior. Some of the differences:

- Real rotors have distributed mass and stiffness
- Rotor construction is more complex
- Press fit components have to be modeled
- There are an infinite number of natural frequencies (modes) and critical speeds
- Destabilizing forces
- Excitation forces
- Bearing damping and stiffness coefficients vary with speed

Figure 8 shows a typical centrifugal compressor cross section. In a compressor, masses include the shaft, impellers, sleeves, thrust collars, shrunk on gear meshes, couplings, etc. Stiffness primarily comes from the pedestal supports, shaft and the bearings. Damping primarily comes from the bearings. Fluid film bearings provide stiffness and damping, and are typically speed and direction dependent. However, seals of all types also have to be considered. Per API-684-1, "…For unbalance response analysis, the API requirement is to include oil seals only." Dry gas seals by comparison do not provide any appreciable damping. Also per API-684-1, "…Toothed labyrinth seals (this includes impeller eye labyrinths, balance piston labyrinths, etc.) are basically neutral in their behavior for unbalance response due to several factors. First, their principal stiffness terms are normally several orders of magnitude less than the bending stiffness of the shaft or the rotor support stiffness. With lower principal stiffness terms, they have little influence on the location of the critical speeds. However, damper seals can have a pronounced effect on the location of the critical speeds as discussed below in the gas annular seal section (see Section 2.6.4)."

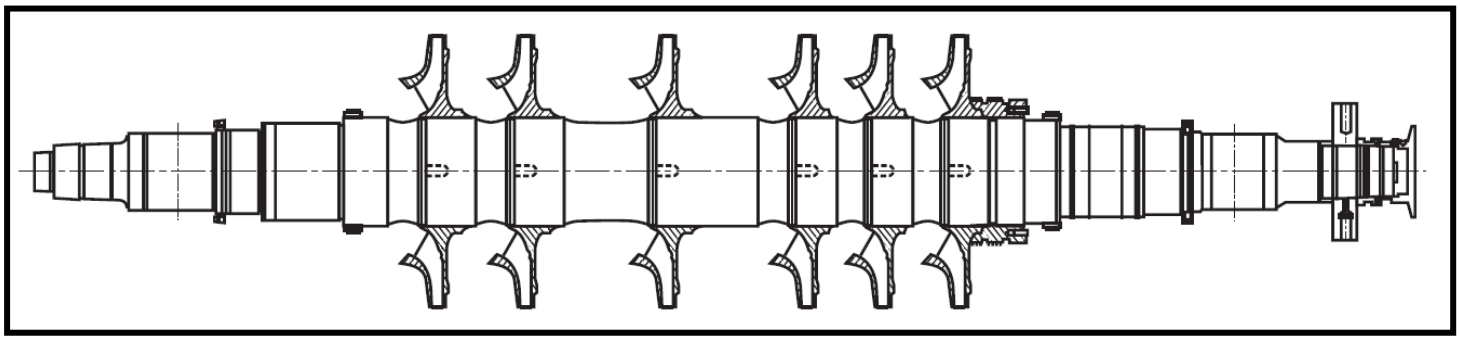

Figure 8: Compressor Cross Section (Courtesy API 684-1)

Regarding the forces, unbalance is typically the dominant lateral disturbing force. It occurs at a frequency of one times the running speed. However, there are other lateral excitation forces such as coupling misalignment, fluid destabilizing forces from bearings and seals, rubs, etc. A good list or potential exciting forces that should be considered can be found in API-684-1, Standard Paragraph SP6.4.1.1.

KEY ELEMENTS OF A ROTORDYNAMIC ANALYSIS

Per API-617, the requirements for lateral rotordynamic analysis reports include:

a) Rotor model
b) Oil film bearings and liquid-film seals data (if present)
c) Rolling element bearing data
d) Bearing pedestal data
e) Gas annular seal data
f) Squeeze film dampers
g) Other forces included in the analysis (machine dependent)
h) Analysis methods
i) Undamped critical speed map and mode shapes
j) Unbalance response predictions
k) Stability level 1 analysis
l) Stability level II analysis
m) Summary sheet that identifies compliance with API requirements

All of this information is important. The key elements are the rotor model, bearing data, undamped critical speed map and mode shapes, damped unbalance response analysis and stability analysis.

ROTOR MODEL

The rotor is modeled as a series of stations connected by mass-less flexible beams. The stations are chosen to coincide with changes in diameters, where there is a concentrated mass such an impeller or thrust collar and at key points like bearing centerlines, seal centerlines and where vibration probes are located. This ends up as a tabulation of the rotor geometry and external masses. API-684-1 provides guidelines on how to model the rotor. This data is important to ensure that nothing in the model was missed and to be able to do an audit or perform and independent rotordynamic analysis in the future to aid in troubleshooting or if a change is made to something in the rotor bearing system. This will actually be covered in Case Study 1.

BEARING DATA

Oil film bearings (and liquid film seals if provided) have stiffness and damping properties. These properties can vary with bearing clearance, oil temperature and speed, which can impact the results of the rotordynamic analysis. For example, as discussed in Smith, Whalen, Benton and Obeid (2019), and in Case Study 1, a small change in clearance changed the frequency of the first critical speed from 7288 CPM to 6615 CPM and also changed the calculated damped magnification factor (also called amplification factor).

Squeeze film dampers have been used in high speed turbomachinery to solve stability and vibration problems that are not easily solved with conventional bearings. In simplest form, the squeeze film damper consists of an inner bearing and an outer bearing. It allows movement between the inner and outer bearings to dissipate the vibration energy. More information on squeeze film bearings can be found in Smith (2010).

It is important that the design preload, bearing clearances (minimum, maximum and design), bearing stiffness and damping coefficients (at minimum, maximum and design clearance) and oil temperature (minimum, maximum and design) are provided. Sometimes the data and calculations are only provided at design and this can be misleading as the rotordynamic behavior at the extremes of bearing clearance and oil temperatures can be very different.

BEARING SUPPORTS

It is also important to consider the bearing pedestal support stiffness and damping characteristics, which act in series with the bearing characteristics. Flexible supports add stiffness with very little damping. With fluid film bearing machines, rigid pedestals have little impact on the lateral rotordynamic analysis. Interested readers can learn more from the paper by Nicholas, Whalen and Franklin (Proceedings of the Fifteenth Turbomachinery Symposium).

The effect of the bearing support stiffness is often overlooked in lateral rotordynamic analysis. For very heavy rotors, machines with flexible bearing supports ($K_{support} < 3.5*K_{bearing}$), or machines where a rigid bearing support model does not accurately reflect operating characteristics, a bearing support model should be included. Several methods have been developed to model support stiffness effects. For existing equipment, the bearing support mass elastic properties can be determined from an impact test with an instrumented hammer. For proposed equipment, a 3D finite element model of the support structure can be used to determine support stiffnesses. This is placed in series with the bearing stiffness and damping coefficients. For machines that can be accurately modeled by assuming rigid bearing supports based on similar designs, the bearing support stiffness effects can be omitted from the model.

UNDAMPED CRITICAL SPEED MAP AND MODE SHAPE

The calculations done in the previous section illustrate the first bending mode but many rotors operate above the first bending critical speed. These are referred to as flexible shaft rotors and have higher order modes that must be analyzed. An undamped critical speed map is a plot of a rotor's undamped natural frequencies versus the combined bearing and support stiffness. Typically, only the first three or four modes are presented in this plot.

A mode shape is the deflected shape of a rotor calculated at the particular natural frequency. Each critical speed will have a different mode shape. The appearance of the mode shapes will depend on the bearing stiffness relative to the shaft stiffness. When the stiffness of the bearings is relatively small compared with the shaft, the lower order mode shapes will tend to look like rigid body modes. In this case, for a rotor supported between bearings, the first mode is usually a translational (bounce) mode, the second mode is usually a conical (rocking) mode, while the third mode is a U-shaped mode, often called the first bending mode. When the stiffness of the bearings is relatively high as compared with the shaft stiffness, the mode shape will primarily depend on the mass and bending stiffness of the rotor. For a between bearing rotor, these modes shapes will look like bending modes like the ones shown on the right side of Figure 9.

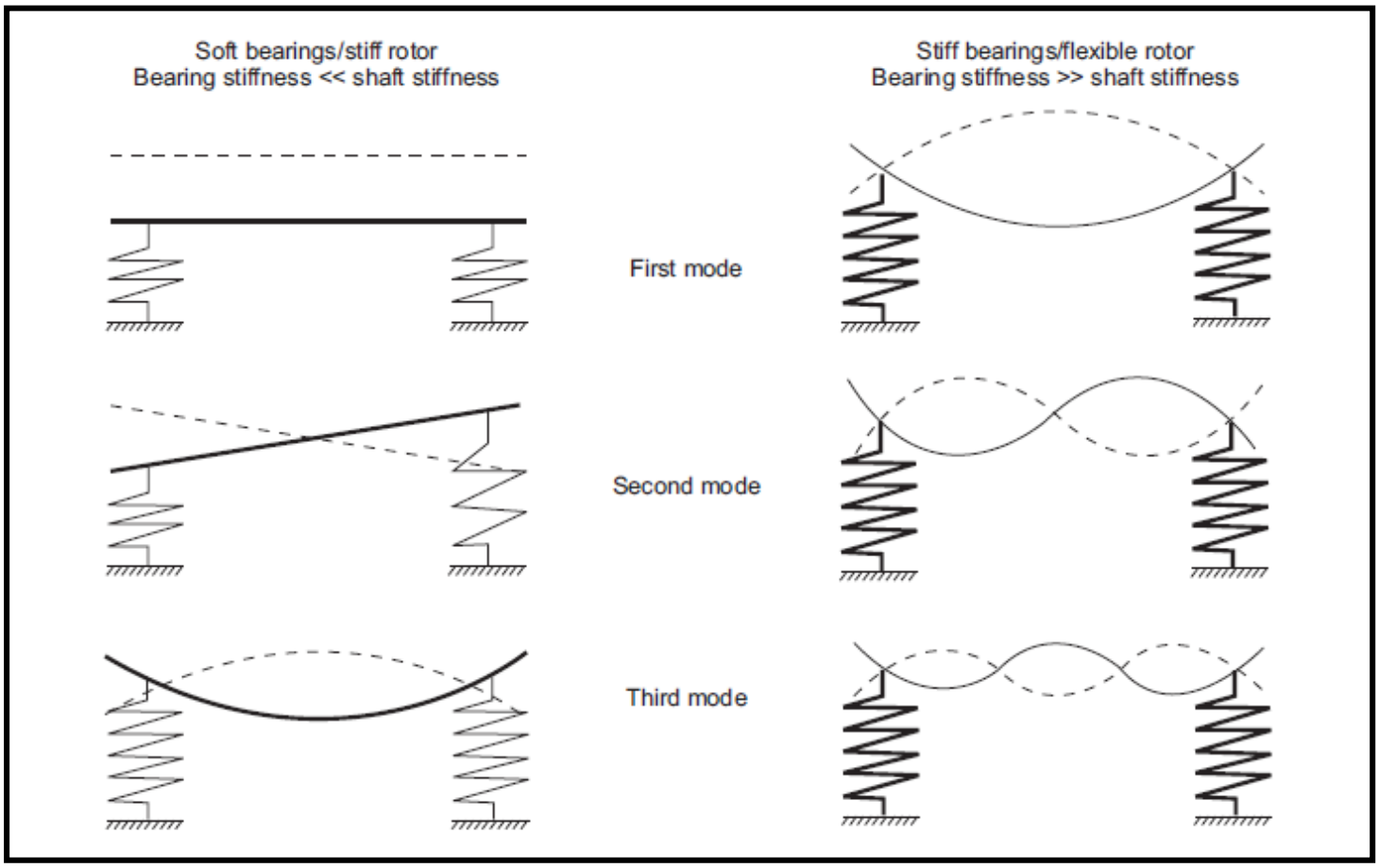

Figure 9: Mode Shapes

A node is a location where the displacement is zero. For the soft bearing rotor on the left side of Figure 8 for example, there is a node in the middle of the rotor for the second mode. As shown, stiffer bearings tend to move the nodes of the mode shapes towards the bearing location. This greatly reduces the ability of the bearing to dampen a critical speed as you need lateral shaft motion at the bearing for damping to occur.

The undamped critical speed map is not used to calculate the final rotor bearing critical speeds because the effects of actual bearing stiffness and damping are not accounted for. Additionally, there is typically no consideration for the bearing support/pedestal effects in the calculation of the undamped critical speeds. However, this initial analysis does provide some indication of the potential damping based on the distance of bearings from nodes in the mode shapes. If a bearing is located on a node then that mode will tend to be unstable. If a bearing is located at an anti node – (large displacement at the bearings) then the mode will tend to be stable.

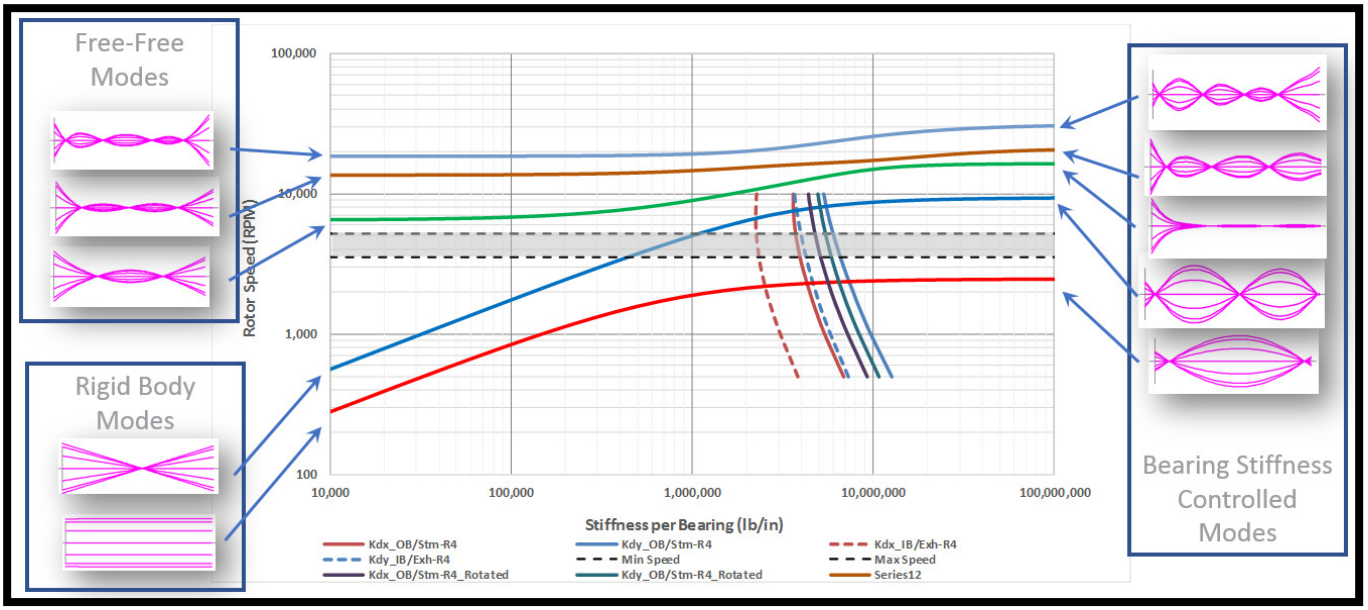

Figure 10: Influence of Bearing Stiffness on Mode Shapes

Understanding the mode shapes is valuable for other reasons too. First, the location(s) of the greatest displacement(s) are places that are the most sensitive to excitation forces for that particular mode. So, when performing the damped unbalance response analysis, unbalance will be located at these locations. For flexible shaft rotors, this includes the lower modes as well as the rotor will have to accelerate through these lower modes, This will actually be discussed in Case Study 5. Second knowing the mode shapes permits an estimation of rotor displacements at close fit areas such as bearing and seal locations, and at vibration probe locations. And understanding the predicted mode shape can help with understanding and troubleshooting a vibration problem in the field. This will be illustrated in Case Study 3.

DAMPED UNBALANCE RESPONSE ANALYSIS

The damped unbalance response analysis uses bearing damping and stiffness coefficients to predict the rotor/bearing system behavior. Outputs from the damped unbalance response analysis include damped critical speeds, amplification factor (AF), separation margin (SM), and predicted amplitude at close-clearance locations (bearings and seals) and probe locations.

A damped unbalanced response analysis is a calculation of the rotor's response to a set of applied unbalances. The applied unbalance excites the rotor synchronously, so the rotor's response to the applied unbalance will occur at the frequency of the shaft's rotation speed. The damped unbalance response analysis should account for all applied steady state linearized forces (bearing and seal stiffness and viscous damping, support effects, and others) and is used to predict the critical speed characteristics of a machine. It is acceptable to exclude the effects of compressor or steam turbine labyrinth seals from the damped unbalance response analysis per API 684.

Imbalance is applied to the rotor model based on the analyst's assessment of the undamped mode shapes. The imbalance location should be selected to excite the modes of interest. This often requires multiple runs with imbalance at multiple shaft stations. The imbalance magnitude is selected per API 684 to be 4*4W/N where W is the journal static load and N is the maximum continuous operating speed (MCOS). Results of this analysis are typically presented in Bodé plots as shown in Figure 11.

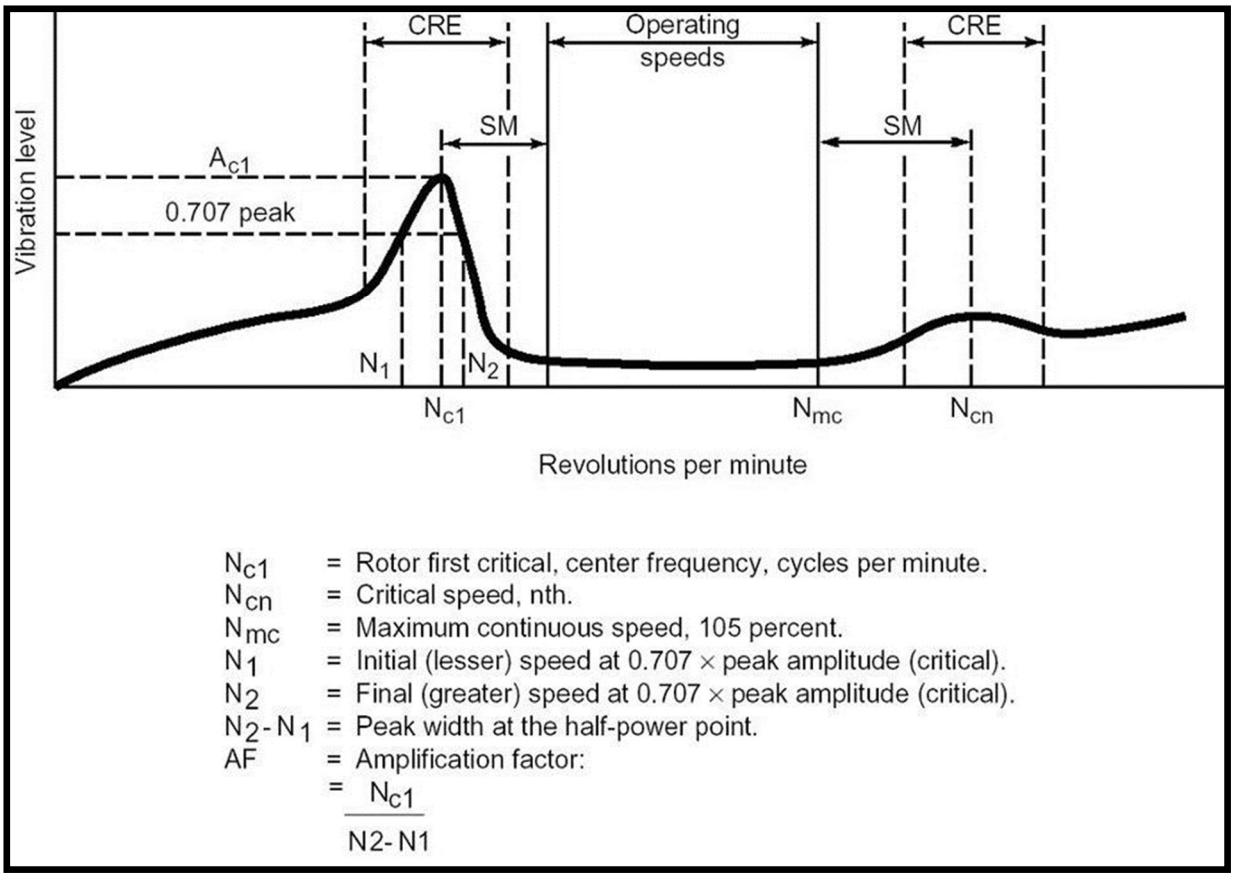

Figure 11: Bode Plot

Bode plots are generated at a specific location on the rotor. Per API-617 Bode plots are generated at the vibration probe locations (or at the bearing centerlines if there are no vibration probes near a bearing centerline). However, Bode plots can also be generated at other areas of particular interest, such as locations of maximum displacement for all applicable modes, critical clearance areas, etc.

The vibration peaks from the Bode plots are the resonant speeds and these peaks are reviewed for the magnitude of the response and the proximity to the operating speed. The magnitude is evaluated based on the amplification factor (AF), which is similar to the magnification factors discussed above. Amplification factor is therefore a measure of a rotor bearing system's vibration sensitivity to unbalance when operated in the vicinity of one of its lateral critical speeds. A high amplification factor indicates that rotor vibration during operation near a critical speed could be considerable and that critical clearance components such as labyrinth seals and bearings may rub stationary elements during such periods of high vibration. The method of calculating the amplification factor is shown on the Bode plot in Figure 9. This also introduces the term called the separation margin (SM), which is the margin of the peak vibration to the operating speed. API defines critical speeds as those resonant speeds with an amplification factor greater than 2.5. If the amplification factor is less than 2.5, no separation margin is required and the natural frequency is not considered a critical speed. If the amplification factor for any natural frequency is above 2.5, that natural frequency is considered a critical speed and a separation margin to the operating speed is required based on the calculated amplification factor. It is therefore important that an accurate analysis is performed since an AF of 2.6 is considered a critical speed.

In addition to evaluation of the amplification factor at critical speeds and the separation margins, the predicted amplitude at close-clearance location should be evaluated. API provides instructions for calculating and applying a correction factor (CF) to the predicted major axis amplitude at close clearance locations. The predicted amplitude at close-clearance locations such as seals is considered acceptable when the major axis amplitude with the correction factor applied is less than 75% of the normal design clearance up to the trip speed for the machine. Note that this requirement does not apply where abradable seals are used.

API also specifies that the damped unbalance response analysis include calculation of the predicted response using bearing coefficients calculated at the minimum, maximum, and design bearing clearance and at the extremes for bearing lube oil supply temperature. This is another often overlooked requirement from the API standards.

STABILITY ANALYSIS

As discussed above, the log decrement is a measure of how quickly the free vibrations experienced by the rotor system decay. When the log decrement is positive, the system is stable. Conversely, when the log decrement is negative, the system is unstable. The log decrement has proved to be a useful measure of rotor stability because it is a non-dimensional quantity and may be interpreted using general design rules. The higher the log dec, the more stable the rotor is.

The log dec is one of the factors used in the stability analysis, which is used to indicate whether there are any self-excited vibration problems in the system such as whirl induced by bearings, seals/shrouds, aerodynamic effects, etc. Stability is a term referring to a unit's susceptibility to vibration at subsynchronous frequencies due to cross coupled/ destabilizing forces produced by stationary critical clearance components (such as bearings and seals). The gases, while passing through narrow passages in the aero-path in the compressor, generate forces on the rotor. Imagine small molecules of the gases passing through the narrow paths, twisting and turning. These molecules have velocity in all the three directions. The tangential velocity is the one that generates the "exciting" forces on the shaft. This is also known as the Swirl velocity. One way to think of cross coupling is that if a force is applied in one direction, say the "x" direction, there will be a response in the "x" and "y" directions. The forces generated by the swirl component can be modeled as cross-coupling stiffness ("Kxy terms").

Based on API-617, the following parameters are used to determine the minimum level of stability analysis:

- Ratio of the calculated cross coupling divided by the minimum cross coupling needed to achieve a log decrement equal to zero
- Log dec
- Critical speed ratio
- Average gas density

UNDERSTAND AND INTERPRET A ROTORDYNAMIC ANALYSIS

While it may be impractical for all engineers tasked with reviewing a lateral rotordynamic analysis report as part of a new equipment purchase or upgrade to understand some of the detailed requirements of the related API standards or be able to describe the subtle differences in the software tools used by OEMs or consultants to produce the results, it is important that they be able to interpret the results, understand the assumptions, and identify deficiencies in the model, processes, or report contents. This section is meant to be a guide for an equipment purchaser or end user to conduct a competent review of a lateral rotordynamic analysis report. It is broken into sub-sections to describe each component of a rotordynamic analysis report and provides a list of questions the reviewer should be able to answer from the report contents. This is not meant to replace the requirements outlined in API 684 but should provide the reviewer an outline for conducting a competent review.

ROTOR MODEL

The most basic part of the lateral rotordynamic analysis that can go wrong is in the model of the rotor geometry. Incorrect dimensions, material properties, or modeling practices can still allow an analyst to produce pretty plots and fill out a boiler-plate type report template. Careful inspection of the following by a reviewer can help mitigate the risk of installing a problem machine built based on incorrect rotor modeling techniques:

Lateral Rotordynamic Analysis Inspection Point: ***Shaft Model***	
Shaft Geometry	Does the overall length of the rotor in the model match that of the subject machine?
	Is the bearing span (axial distance between bearings) identified and correct?
	Does the total mass of the rotor assembly match other documentation from data sheets or inspection reports?
Disks	Are the disks (impellers, turbine wheels, etc.) at the correct axial location?
	Are the disk mass and transverse inertia values included and correct?
	Are all attachments accounted for (coupling half weight, shaft sleeves, disks, etc.) correctly?
Miscellaneous	Are the probe locations identified correctly?
	Are the lengths of elements in the model appropriate with a length to diameter ratio (L/D) between 0.1 and 0.5?
	Are the shaft and sleeve material property assumptions stated in the report and do they account for actual material and normal operating temperatures?

BEARING MODEL

Fluid film bearing stiffness and damping coefficients used in lateral rotordynamic models may be included based on published test data, interpolation of bearing tabular data for similar designs, calculated from dedicated fluid film bearing codes, or determined from detailed computational fluid dynamics (CFD) commercial codes. There are a number of commercially available bearing codes that have been proven to produce satisfactory coefficients when applied properly for most machines. The inclusion of more variables in the analysis such as pad or pivot deflection due to thermal or elastic loads or a detailed model for lubricant admission to the bearing may be required in some cases but superfluous in others. The report reviewer should question the analyst on whether the code used to calculate bearing coefficients can consider these things. In all cases, when the results from an analysis do not match measured performance on a test stand or in the field, a more detailed bearing model or application of a different bearing code capable of including these phenomena may help to identify the source of the discrepancy between predicted and actual performance. Regardless of the code used for determining bearing coefficients, the following set of questions provide a partial list of items a report reviewer should consider before final acceptance of a lateral rotordynamic analysis report:

Lateral Rotordynamic Analysis Inspection Point: ***Bearing Model(s)***	
Bearing Geometry	Is the correct clearance used and stated in the report (radial or diametral)?
	Are the pads located correctly (Load-on-pad vs. Load-between-pad)?
	Is the pad preload stated in the report and correct?
	Were coefficients calculated and provided in the report for the nominal clearance and the range of clearances/preload based on manufacturing tolerances?
	Was the flexibility of the bearing housing/pedestal/support structure considered?
Lubricant	Is the correct lubricant used in the calculation of the bearing coefficients?
	Was the nominal lube oil supply temperature and the acceptable range of supply temperatures considered in the model?
	Does the model used account for the change in lubricant viscosity with temperature?
Loading	Are all static loads accounted for including gravity load, gear transmission forces, steam admission forces, etc.?
	Does the bearing static load change with operating conditions (speed, power, etc.)?
Miscellaneous	Was an appropriate speed range and speed interval considered in the calculation of bearing coefficients?
	Are the bearing coefficients included in the report in graphical or tabular format?

SEAL MODEL

Multistage centrifugal compressors normally have several annular seals to separate regions of high and low pressure and to minimize leakage between stages. Annular gas seals or oil seals are used to prevent the process fluid from discharging into the atmosphere. Compressor interstage and impeller eye seals are usually labyrinth seals with multiple stationary or rotating teeth (or both in the case of interlocking seals) designed to create a tortuous path for the flow and minimize leakage. Seal locations where a high differential pressure is found such as a balance piston or center division wall may be a damper seal design such as a hole-pattern or honeycomb seal. Labyrinth seals are treated as a second order effect in the damped unbalance response analysis and often have a negligible effect on the damped critical speed and predicted amplitude in the forced response analysis. It is important to include gas annular seal effects in the model when evaluating rotor stability due to the relatively high destabilizing cross-coupled stiffness generated in labyrinth seals.

If oils seals are used, their influence on the unbalance response and stability should be evaluated. Dry-gas seals have negligible stiffness and damping that is typically omitted from a lateral rotordynamic model. The mass of the seal sleeve assembly and rotating components should be included in the rotor model.

Lateral Rotordynamic Analysis Inspection Point: ***Seal Model(s)***	
Seal Geometry	Is the correct clearance used and stated in the report (radial or diametral)?
	Are the tooth locations correctly accounted for (tooth on rotor, tooth on stator, or interlocking)?

	Are any special features included in the seal design and were there correctly accounted for in the model (swirl brakes, shunt injection, etc.)?
Fluid Properties	It the correct pressure differential used?
	Are the gas properties assumed for the analysis stated in the report and correct?
	Are any other operating conditions relevant to the study results that need to be evaluated (temperature, pressure, gas composition, etc.)?
Code Capabilities	Were seal effects included in the damped unbalance response analysis? If not, does the report state why they were neglected?
	Are the seal coefficients included in the report in graphical or tabular format?

UCS ANALYSIS

The undamped critical speed analysis is used to determine the undamped critical speeds and mode shapes. This provides some indication of the location of critical speeds to be determined in the damped forced response analysis but, more importantly, provides the analyst guidance on mode shapes and how to correctly apply unbalance (location and phase relationships) to the model in the damped forced response analysis.

Lateral Rotordynamic Analysis Inspection Point: ***UCS Analysis***	
UCS Map Contents	Are undamped critical speeds are plotted as a function of support stiffness with suitable ranges in bearing stiffness?
	Are the predicted bearing stiffnesses overlaid on the UCS Map?
UCS Mode Shapes	Are the UCS mode shapes plotted?
	Were the UCS mode shapes consulted to determine unbalance distribution in the damped unbalance response analysis?

DAMPED FORCED RESPONSE ANALYSIS

The damped forced response analysis is the primary output of a lateral rotordynamic analysis report for identifying the location of damped critical speeds, their amplification factors, and predicted amplitude of the response. Some common deficiencies in reports include incorrectly applying unbalance (location or phasing) to excite a critical speed mode shape or incorrectly assessing the predicted amplitude.

Lateral Rotordynamic Analysis Inspection Point: ***Damped Forced Response Analysis***	
Assumptions	Are the locations of applied unbalance clearly identified and correct for the mode shapes under review?
	Is the magnitude of the imbalance applied correctly calculated and stated for each load case?
Output Plots	Was the response evaluated from 0-125% of the trip speed?
	Was a reasonable speed increment used to properly locate critical speeds and calculate the amplification factor at critical speeds?
Acceptance Criteria	Is the required separation margin for a critical speed met in accordance with API standards?
	Is the maximum predicted amplitude compared to available clearance and found to be acceptable?

STABILITY ANALYSIS

Deficiencies in the stability analysis section of a lateral analysis report are often in the assumptions used to quantify destabilizing cross-coupling magnitude. API provides guidance on this for a Level I stability analysis. For a Level II stability analysis, careful consideration of both the assumptions for inputs to codes used to calculate rotordynamic coefficients used in the analysis and the capabilities of the codes. There are many codes commercially available that may provide adequate results. However, when the predicted stability of the rotor-bearing system does not replicate the stability of the system observed on a test stand or in the field, a more advanced code or careful review of assumption is prudent.

Lateral Rotordynamic Analysis Inspection Point: ***Stability Analysis***	
Assumptions	Was the destabilizing cross-coupling applied at the correct location in the model?
	Was the destabilizing cross-coupling correctly calculated and the assumed magnitude stated in the report?
Acceptance Criteria	Were the requirements of the Level I stability analysis met? If not, was a Level II stability analysis conducted?
	Were all destabilizing components considered in the Level II analysis (if conducted)? Does the report clearly state all assumptions for the seal rotordynamic coefficients?

EXAMPLES OF DEFICIENCIES IN REPORTS THAT CHANGES THE ANALYSIS

The authors have completed and/or evaluated multiple lateral rotordynamic analyses over the years and have seen how failure to adhere to good engineering practices and blindly relying on an OEM or consultant to say that a machine is acceptable can lead to poor results. This may be caused by poor assumptions, lack of competence of the analyst, relying too heavily on software tools without stopping to question if the results produced make sense, or a simple copy and paste error. Regardless of the source of inaccuracy, the consequences can be costly.

As an example of a failure to adequately apply good engineering judgement and accepted standards, forced response analysis results from a lateral rotordynamic analysis conducted by an aftermarket vendor as part of a compressor re-rate project are shown in the left hand side of Figure 12. The vendor only calculated the forced response analysis at the minimum and maximum operating speed. A third-party analysis identified a critical speed in the operating speed range using a more suitable speed increment (right side of Figure 12). Needless to say, such an oversight could have resulted in excessive vibration amplitude for the subject machine due to the presence of a critical speed within the normal operating speed range.

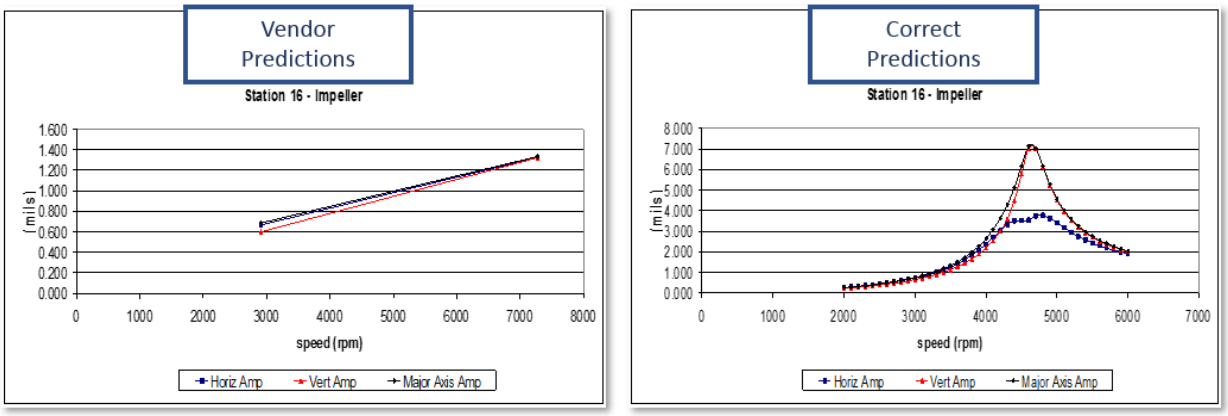

Figure 12: Improper Speed Increment for Forced Response Predictions

Another example of questionable results was identified in a third-party review of an OEM rotordynamic analysis conducted during a compressor re-rate. A third-party review found a discrepancy in their calculated bearing coefficients when compared to those in the OEM report. At higher rotor speeds, the third-party predictions resulted in much lower direct stiffness and damping compared to the OEM report. After some additional review, it was determined that the OEM analyst used a constant viscosity model for the bearings. The third-party was able to duplicate the OEM results using a constant viscosity model. This method does not consider the change in the lubricant viscosity as the temperature increased. This could result in under-predictions of critical speeds near the upper end of the speed range and over-predicting their amplification factors.

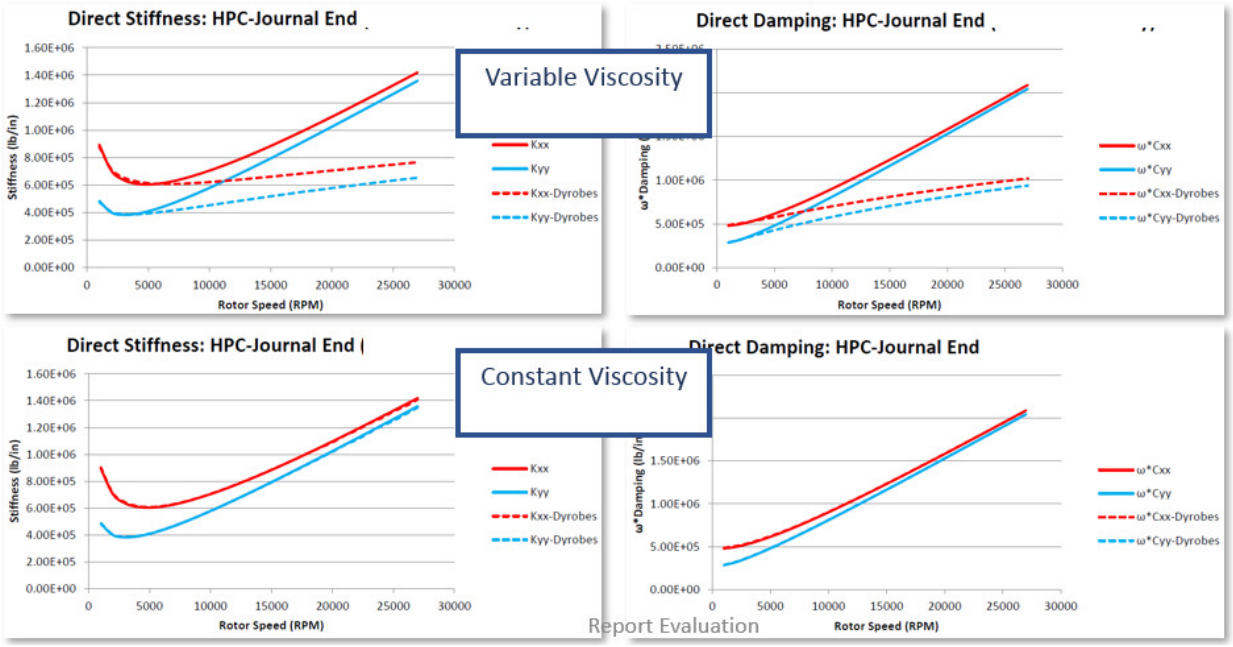

Figure 13: Calculated Bearing Coefficients using a Variable and Constant Viscosity Model

Now let's look at some examples of where rotordynamics were used to identify and solve problems in the field or on the test stand.

CASE STUDY ONE

This case study pertains to an integrally geared centrifugal compressor driven by a 5,000 HP, 1,794 RPM induction motor. The gearbox consists of a bullgear and three rotors. The stage one/two rotor consists of a pinion with overhung impellers mounted at both ends while the stage three rotor consists of a pinion with a single overhung impeller. These rotors are mounted at the horizontal split line. The stage four/five rotor is in the top of the gearbox cover and consists of a pinion with overhung impellers at both ends.

The gearbox utilizes tilting pad journal bearings for all three pinions with "X" and "Y" non-contacting proximity type shaft vibration probes adjacent to each bearing. The pinions are fitted with thrust collars which transmit pinion axial thrust to the bullgear. The bullgear rotor is fitted with a sleeve type journal bearing on the drive end and a combined sleeve type journal bearing and tapered land type thrust bearing on the non-drive end. The pinion bearings are all fitted with temperature probes mounted just below the babbitt surface on the loaded pads. The compressor control system includes high vibration alarms, high vibration shutdown protection and high bearing temperature alarms. The gearbox arrangement for stages 1 to 3 is shown in Figure 14; the stage four/five rotor is omitted for clarity.

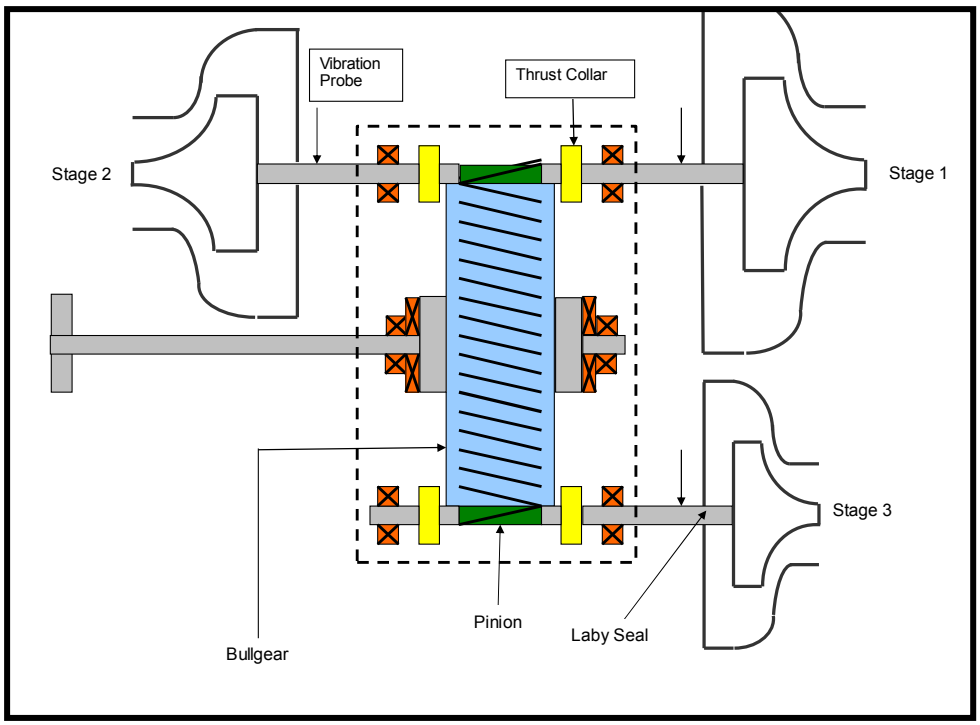

Figure 14: Compressor Arrangement for Case Study One (Stage Five/Six Rotor Not Shown)

To address problems with high bearing temperatures on the stage one/two compressor rotor, these bearings were replaced with modified bearings with a larger assembled clearance. This was successful in lowering the bearing temperatures from over 250°F (121°C) to approximately 170°F (77°C) to 180°F (82°C). The assembled design radial clearance was increased from 2.6 mils (0.066 mm) to 4.4 mils. Note that the pad clearance was also changed to maintain a similar preload.

When making a bearing design change, the bearing damping and stiffness will also change. Table 1 shows the differences the bearing stiffness and damping coefficients for both the original design and the modified design. The impact of this change on the rotordynamic behavior can be seen in the damped unbalance response analysis. For this case study, damped unbalance response plots were generated at the following locations:

- Station 1: second stage impeller
- Station 11: second stage bearing
- Station 20: rotor mid-span
- Station 29: first stage bearing
- Station 39: first stage impeller

CASE	CLEARANCE	Pad Radial Clearance inches	Assembled Radial Clearance inches	PRELOAD	STIFFNESS		DAMPING	
					KXX lbf/in	KYY lbf/in	DXX lbf-sec/in	DYY lbf-sec/in
Original	Design	0.0037	0.0026	0.291	8.71E+05	1.39E+06	6.10E+02	6.65E+02
Original	Maximum	0.0037	0.0036	0.018	6.46E+05	1.37E+06	3.18E+02	6.17E+02
Modified	Minimum	0.0063	0.0040	0.364	6.12E+05	1.10E+06	2.74E+02	4.09E+02
Modified	Nominal	0.0063	0.0044	0.304	5.60E+05	1.07E+06	2.48E+02	3.77E+02
Modified	Maximum	0.0063	0.0048	0.237	5.21E+05	1.04E+06	2.34E+02	3.72E+02

Table 1: Case Study One Bearing Data

Figures 15 and 16 show the difference in the Bode plots for one of the unbalance cases that was analyzed.

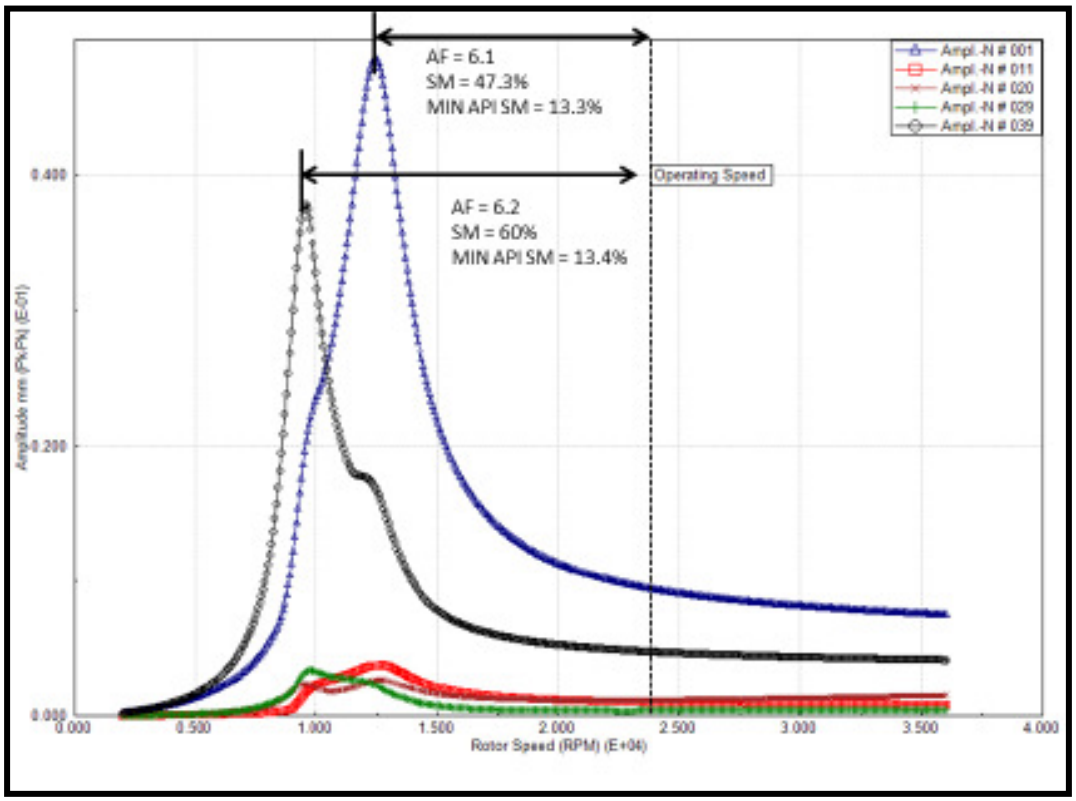

Figure 15: Unbalance Response; Original Bearing Clearance

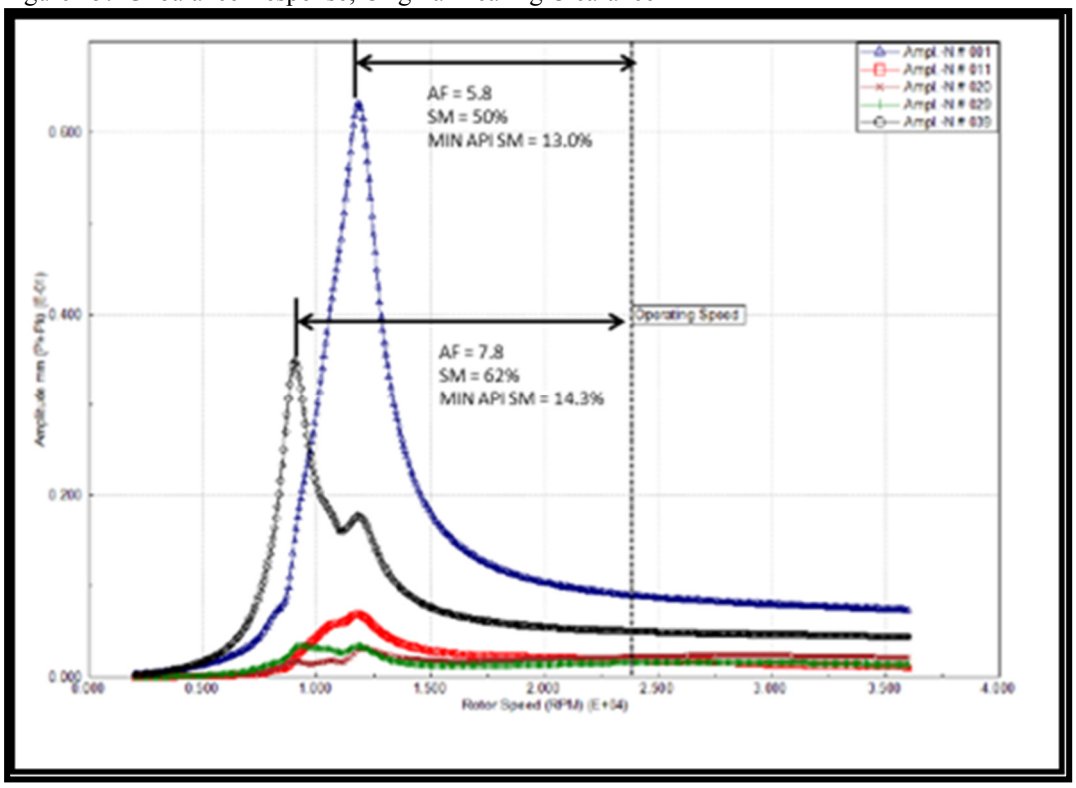

Figure 16: Unbalance Response; Modified Bearing Clearance

The results of the damped unbalance response analyses for both the original bearing clearance case as well as the modified bearing clearance case are shown below in Tables 2 and 3.

MODE #	ORIGINAL DESIGN BEARING CLEARANCES					
	Natural Frequency CPM	Critical Damping Ratio	Log Dec	Amplification Factor	Separation Margin	API Required SM
1	7288	0.0604	0.38	8.3	69%	16%
2	9531	0.1013	0.64	4.9	60%	16%
3	10395	0.0703	0.44	7.1	56%	16%
4	12386	0.0851	0.53	5.9	48%	16%
5	54281	0.0558	0.35	9.0	128%	26%
6	67580	0.1577	0.99	3.2	183%	26%

Table 2: Results of Damped Unbalance Response Analysis for Original Diametral Bearing Clearance Case

MODE #	MODIFIED BEARING CLEARANCES					
	Natural Frequency CPM	Critical Damping Ratio	Log Dec	Amplification Factor	Separation Margin	API Required SM
1	6615	0.0654	0.41	7.6	72%	16%
2	8535	0.0727	0.46	6.9	64%	16%
3	9724	0.0561	0.35	8.9	59%	16%
4	11554	0.0851	0.53	5.9	52%	16%
5	20336	0.4072	2.56	1.2	15%	0%
6	27023	0.4501	2.83	1.1	13%	0%
7	36812	0.2838	1.78	1.8	54%	0%
8	51447	0.3998	2.51	1.3	116%	0%

Table 3: Results of Damped Unbalance Response Analysis for Modified Diametral Bearing Clearance Case

What is interesting is that what may be viewed as a relatively minor increase in bearing clearance had a moderate impact on the calculated natural frequencies (10% reduction for mode one) and the stability (8% increase in mode one log dec). Based on the original design case, there were no natural frequencies near the operating speed. With the modified clearance case there are 2 modes (modes 5 and 6) which are close to the operating speed. Fortunately, these modes are very well damped. While there are no stability issues for either case, the magnitude changes show the value in considering this analysis anytime a change is made to something in the rotor/bearing system.

CONCLUSIONS FOR CASE STUDY ONE

While the lateral rotordynamics for both the original bearing clearance case as well as the modified bearing clearance case were acceptable per API-617 standards, the analyses do show that the rotordynamic behavior changes even when making what appears to be a minor bearing clearance change. And for this reason, a lateral rotordynamic analysis should be considered whenever something is changed in the rotor bearing/system.

CASE STUDY TWO

This case study involves a large centrifugal compressor in charge gas service in an ethylene plant. The unit was running fine when a power outage shut the plant down. The train came down fine but when brought back up it was noted that one bearing exhibited high levels of vibration.

This is the low pressure “A” case compressor located between the steam turbine driver and a gearbox which drives the medium pressure “B” case compressor. Alarm and trip levels were set to 3 and 5 mils respectively, and the compressor normally runs around 4750 rpm. The bearing in question is a 6-inch 5 pad load between pad (LBP) bearing with an L/D ratio of 0.5 loaded to 225 psi.

The low-pressure compressor outboard bearing vibration had increased from under 1 mil of vibration pre-outage to over 5 mils vibration after coming back up; this vibration was substantially synchronous, had a forward precession, a round orbit and was speed dependent, there was also a slight phase shift. All of this (and other data, history, and condition analysis) pointed to a balance condition change on that end of the machine.

There was a lot of speculation on how the rotor became unbalanced however rotordynamic analysis indicated only a coupling

unbalance (or other similar synchronous forcing function) could cause the vibration levels observed.

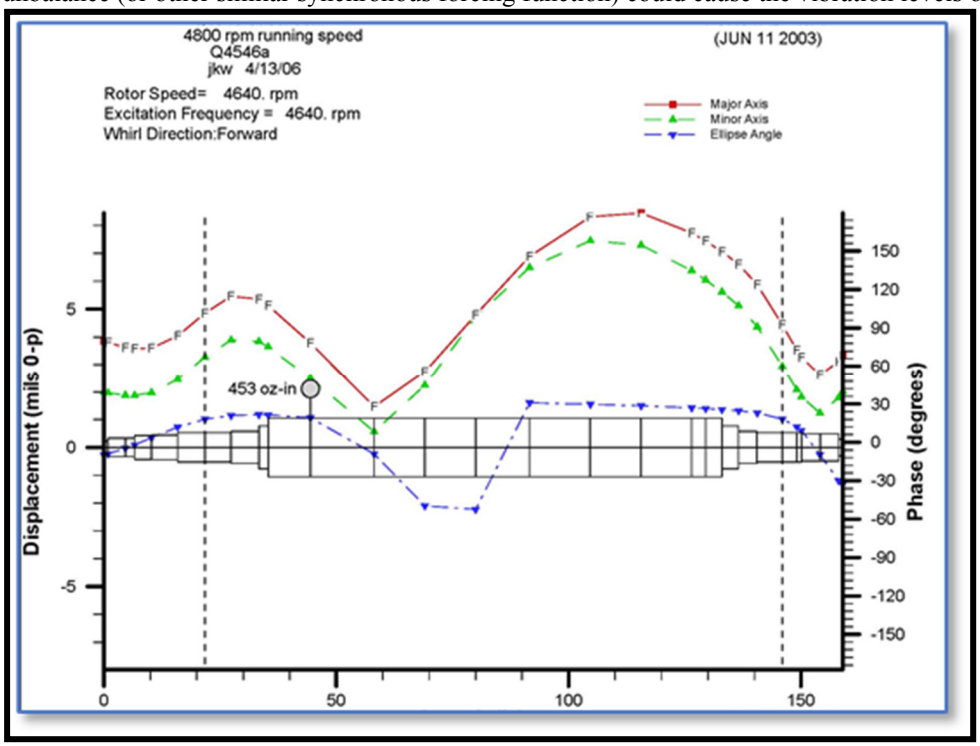

Figure 17 Rotor deflection due to imbalance

The rotor deflection shape from an unbalance at the first impeller (impeller closest to the bearing experiencing the high vibration) is presented in Figure 17. Note that this is a drive though machine so there is a coupling on each end. Also note that the analysis predicts that for this unbalance the vibration at each bearing should be about the same. However, the actual machine had 5 mils vibration on one bearing and 1 mil on the other. It was determined that an unbalance between bearings could not duplicate the vibration spread observed.

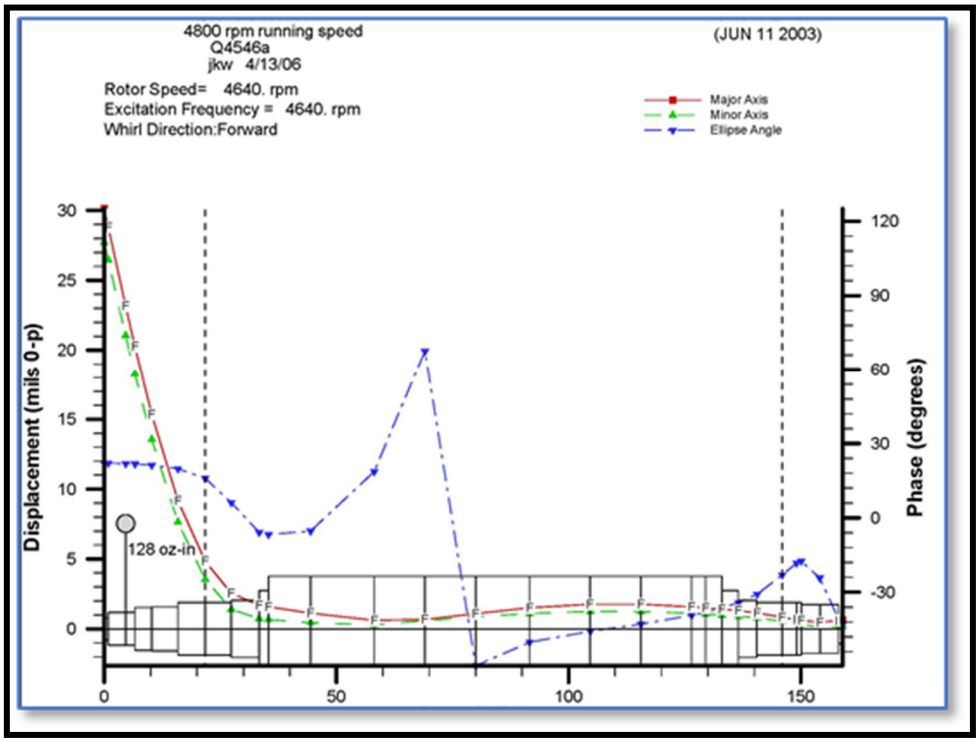

Figure 18 Rotor deflection shaft with coupling unbalance

As shown in Figure 18 when applying an unbalance to the coupling we find the roughly 5 to 1 variation in vibration as observed from one end of the rotor to the other. It was determined that somehow the coupling became unbalanced – even though the vibration on the

other side of the coupling remained low. This analysis also replicated the speed dependency found in the actual machine.

Now the focus shifted to determine if continued operation would lead to an unplanned shutdown due to bearing failure.

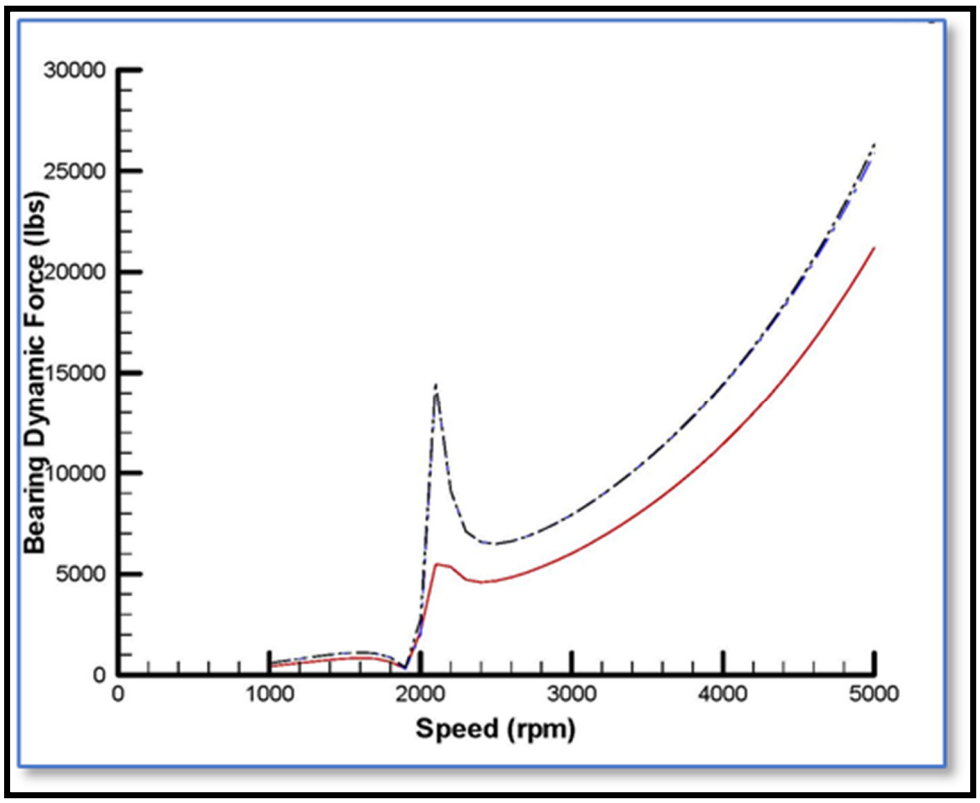

Figure 19 Bearing force due to coupling unbalance

The dynamic force imparted on the bearing due to a coupling unbalance sufficient to raise the vibration to 5 mils is depicted in Figure 19. Note the significant dynamic load (which is zero to peak). The bearing had (roughly) a static load (journal load) of 4000 pounds and a dynamic load of +/- 20,000 lbs.

Analysis of the steady state condition of the machine predicted a maximum film pressure of 750 psi so one could estimate that the dynamic pressure was 3750 psi. Analyzing this as a compressive stress of 750 psi and an alternating stress of 3750 psi we can then look at the babbitt compressive strength at 180 °F of 4000 psi (see Figure 4) and realize we are very near failure.

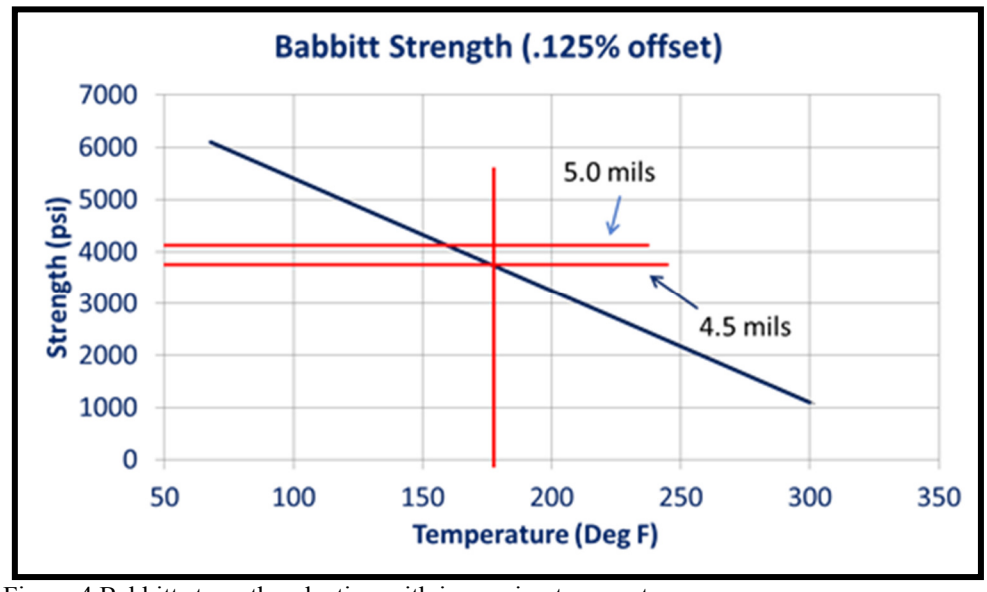

Figure 4 Babbitt strength reduction with increasing temperature

It was decided to reduce speed to maintain vibration levels at or below 4.5 mils and continue to run. This of course resulted in reduced plant output put did allow the machine to continue to run. Financial analysis dictated that they run for another 3 years under this constraint. The bearing health was monitored by observing shaft centerline data, bearing temperature readings, and performing frequent oil analyses.

An alignment consultant was brought in and determined that there was an offset misalignment that would have presented itself as a synchronous force on the rotor. When the machine came down, they found that the coupling had spun and friction-welded itself to the rotor – this caused the misalignment and change in balance condition. It was theorized that there may have been a significant liquid ingestion when coming back up after the power outage.

What did this bearing have going for it that allowed continued operation for 3 years under this extreme dynamic loading condition? The OEM bearing was replaced a long time ago with a bronze and babbitt bearing with ball & socket (B&S) pivots. The B&S pivots deteriorated very little over this run thanks to the significantly lower stresses compared to other pivot designs. The user is convinced they would not have been able to run this long under these conditions with the originally supplied bearings. The fact that the bearing was running at only 180 °F was also a major factor as this meant the babbitt strength was still relatively high.

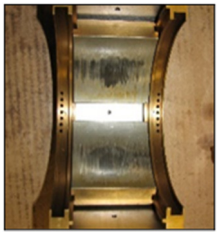
Figure 20

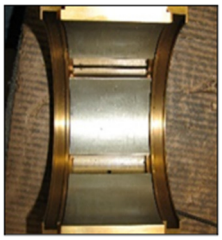
Figure 21

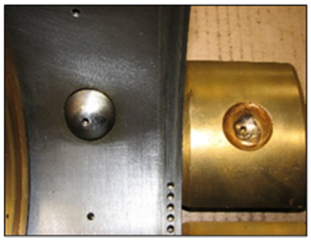
Figure 22

The bearings were removed and inspected, and it was found that the lower two pads had opened up about 2.0 mils due to some pivot wear and babbitt loss. Figure 20 shows the bottom two pads; Figure 21 the top pads Figure 22 is a close up of the pivot wear. The bearing on the other end had the same bore as when it shipped 11 years earlier.

The rotor, bearings and coupling were replaced and the machine came back up with vibration levels on both ends under 1 mil.

CASE STUDY THREE

Case study three pertains to a five stage integrally geared centrifugal compressor driven by a 2976 RPM, 6800 KW induction motor. The gearbox consists of a bullgear and three rotors. The gearbox utilizes tilting pad journal bearings for both pinions with “X” and “Y” non-contacting proximity type shaft vibration probes adjacent to each bearing (except for the free end of the cover rotor which has only one vibration probe.

The motor utilizes sleeve type radial bearings on both the drive end and non-drive end with “X” and “Y” non-contacting proximity type shaft vibration probes adjacent to each bearing. There are no thrust bearings in the motor. The motor protection system includes high vibration alarm and high vibration shutdown protection.

The coupling is a disc pack type with an extended spacer. The spacer subassembly consists of coupling hubs at both ends that are shrunk fit onto the bullgear and motor shafts. Adapter plates are bolted to the hubs which are then bolted to the spacer through the disc packs. Because of the length of the spacer, it was made in two parts that are bolted together in the middle of the assembly. A picture of the coupling shown in Figure 23.

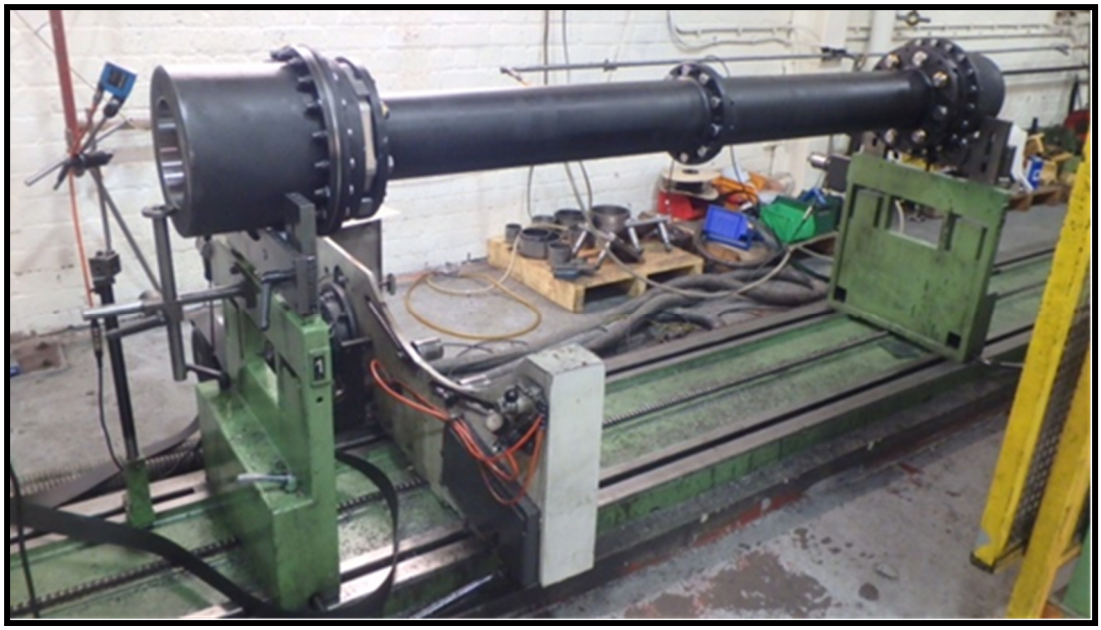
Figure 23: Case Study Three Main Drive Coupling

COMMISSIONING

When the motor was run uncoupled in the field for the first time, the drive-end (DE) shaft vibration levels were 2 mils p-p (51 microns) and 1.5 mils p-p (39 microns), while the non-drive-end (NDE) vibration levels were 0.5 mils p-p (12 microns) and 0.7 mils p-p (19 microns). The DE shaft vibration level was slightly higher than the typical API limit of 2.0 mils p-p (50 microns) for a motor of this design and speed. When the motor was coupled to the compressor, the DE vibration levels increased to 6.1 mil p- (157 microns) and 4.0 mils p-p (103 microns) while the NDE vibration levels were essentially unchanged. The NDE coupled vibration levels also increased about 0.39 mils p-p (10 microns) to 0.79 mils p-p (20 microns) when the load was increased. The vibration could be felt on the motor foundation and loud noises were reported coming from the motor.

A spectrum analyzer was connected to the vibration transmitters to measure the spectrums and view the shaft orbits. This showed that the vibration was predominately at frequency of one times running speed. It also showed that a banana shaped DE orbit and a circular shaped NDE orbit.

A review of the motor rotordynamics showed that the motor was a flexible shaft design that operated above the first bending critical speed of about 1650 CPM. It also showed no lateral or torsional natural frequencies near the operating speed. Since the high vibration only occurred on the DE and only when the motor was coupled to the compressor, misalignment or coupling unbalance were considered likely causes of the high DE vibration.

It was clear that the vibration levels were excessive and there was a real risk of a motor mechanical failure if the compressor were put into continuous operation. The author experienced a violent failure of a similar sized motor that ran at high vibration levels for an extended period. So, it was decided that the vibration issue had to be resolved before the compressor could be put into service.

ALIGNMENT

The compressor gearbox is mounted on a large structural steel frame. The thermal growth of the compressor, frame and motor were reviewed based on measured data to determine if the original cold vertical offset used for the motor/compressor alignment was correct. A hot alignment was also checked to validate this. Based on the analysis, it was determined that the motor needed to be lowered by approximately 0.03 inches (0.78 mm). Based on this, it was considered plausible that misalignment may have caused or contributed to the problem and so the motor was lowered to improve the hot alignment.

After the re-alignment was completed, the motor was restarted. Unfortunately, the motor vibration didn't improve and the DE vibration increased slightly to 7.5 mils p-p (190 microns). This shifted the focus to the coupling.

COUPLING BALANCE

The coupling manufacturer followed a multi-stage balancing program for flexible disc couplings in accordance with ISO 1940 G2.5. Motor-end and gearbox-end hubs each underwent single-plane balancing to G1 criteria, followed by a two-plane assembly balance within full G2.5 criteria. The coupling assembly was then balanced on a standard hard-bearing rig, supported radially by rollers and driven by a belt. However, the coupling was only low speed balanced. The motor half coupling hub mass is 190 pounds (86 kg) and the spacer/transmission mass is 672 pounds (305 kg).

The motor manufacturer performed a two-plane balance on the motor rotor in accordance with ISO 1940 G1.0. The motor rotor weighs 4956 pounds (2250 kg). The motor bearing journal diameters are 6.3 inches (160 mm) with a diametral design clearance of 9.4 mils (240 microns). The DE vibration levels during the shop test were 1.1 mils p-p (26.7 microns) and 1.0 mils p-p (25.7 microns) and the NDE vibration levels were 0.7 mils p-p (16.8 microns) and 0.8 mils p-p (20.0 microns).

Table 4 shows a summary of the vibration data:

LOCATION	SHOP TEST, MILS P-P	FIELD – UNCOUPLED, MILS P-P	FIELD - COUPLED LOW POWER, MILS P-P	FIELD - COUPLED NORMAL POWER, MILS P-P
DE - X	1.0	2.0	6.2	7.0
DE -Y	1.0	1.5	4.1	4.5
NDE - X	0.7	0.5	0.9	1.3
NDE - Y	0.8	0.8	0.8	1.3

Table 4: Motor Vibration Summary Case Study Three

The motor was supposedly shop tested with the motor half coupling hub installed. However, this was not consistent with the field data. It appeared that there could be some coupling unbalance.

Due to the need to put the compressor into service it was decided to field balance with the motor coupled to the compressor. Washers were used as balance weights and were added to the motor side coupling hub at the adapter plate bolted connection. There were some initial difficulties field balancing which will be explained in more detail later in this tutorial. However, field balancing was successful in reducing the coupled DE "X" and "Y" motor vibration levels at load to 2.4 mils p-p (60 microns) and 2.0 mils p-p (50 microns). These levels were deemed low enough to put the compressor into operation.

However, the vibration levels were still higher than desirable and field balancing would be required in the future if the coupling was replaced. The suspected cause was coupling unbalance. The successful field balance was accomplished by adding 2.96 ounces (84 grams) at a radius of approximately 6.59 inches (167.5 mm). These equates to a correction of 19.51 ounce-inches (14,070 gram-mm), which is about 10 times the manufacturer's maximum allowable unbalance at the coupling end. So, for coupling unbalance to be the cause, there would likely to have been a problem with the original coupling balance.

There was a spare coupling already being manufactured for this train and the coupling balance was witnessed to ensure there were no questions about the balance. Later on when this new coupling was installed in the field, vibrations were checked at several steps as shown in Table 5.

LOCATION	NO COUPLING HUB, MILS P-P	WITH COUPLING HUB, MILS P-P	COUPLED LOW POWER, MILS P-P
DE - X	<1.1	2.2	3.1
DE -Y	<1.1	1.7	1.6
NDE - X	<0.8	<0.8	<0.8
NDE - Y	<0.8	<0.8	<0.8

Table 5: Motor Vibration During Spare Coupling Installation Case Study Three

With the new coupling installed, the DE vibration levels improved, but there was a significant increase in vibration when the coupling hub was installed and the vibration was still too high after the coupling was installed. So, another field balance was performed. However, the technician performing the field balance struggled. After eight attempts, the motor vibration had not improved and was worse than the starting values. To better understand this and the vibration behavior an independent rotordynamic analysis was performed since a report not available from the motor manufacturer.

ROTORDYNAMIC ANALYSIS

The motor rotordynamic model is shown in Figure 24. Damped unbalance response analyses were performed based on unbalances at the coupling, DE and NDE cooling fans and in the middle for the rotor core. Analyses were performed with and without the coupling to determine the influence of the coupling on the rotordynamic behavior.

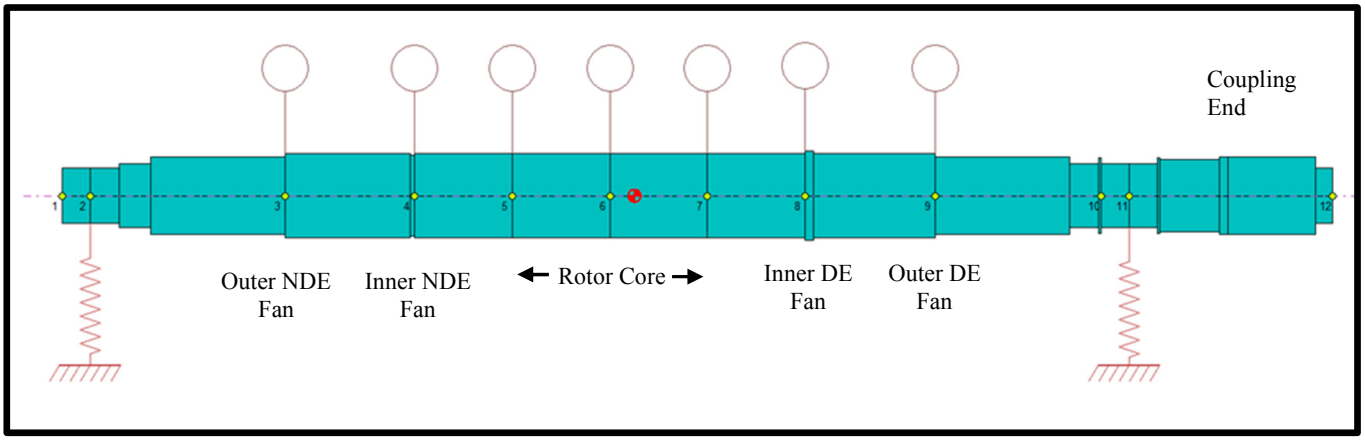

Figure 24: Case Study Three Motor Rotor Model

The mode shape for the second mode is the one of interest since the motor operates above the first bending critical. This mode shape is shown in Figure 25. This includes the mass of the motor coupling hub and half the mass of the spacer/transmission unit. Rotordynamic behavior is a function of the unbalance distribution along the rotor and this is not known. However, when looking at the mode shape, locations where there is a large deflection are more sensitive to unbalance than areas where there is little deflection. As shown in Figure 25, there is a large deflection at the coupling, making this area much more sensitive to unbalance at running speed than at the DE bearing or even the middle of the rotor. That is not to say these other areas can be ignored because the rotor still needs to accelerate and decelerate through the critical speed on every start-up and shut-down. But these areas are good locations for balance planes when the rotor is at running speed. It is also important to know where vibration is being measured when looking at the mode shape. In this case, an unbalance at the coupling end will result in a higher response at the coupling than where the vibration is being measured. Additionally, the rotor deflection at the vibration probe is in phase with the coupling. Had the vibration probe been on the other side of the bearing, the vibration at the coupling and at the probe would have been 180° out of phase. The balance technician had trouble balancing the rotor because he incorrectly assumed that since this is a flexible shaft rotor that the balance weights needed to be added 180° out of phase with the measured phase. Once this was recognized, there was no trouble field balancing. To balance the motor rotor with the spare coupling, a total of 1.12 ounces (31.5 grams) was added at the coupling, which still equates to about 3.7 times the ISO 1940 G2.5 balance limits for the coupling.

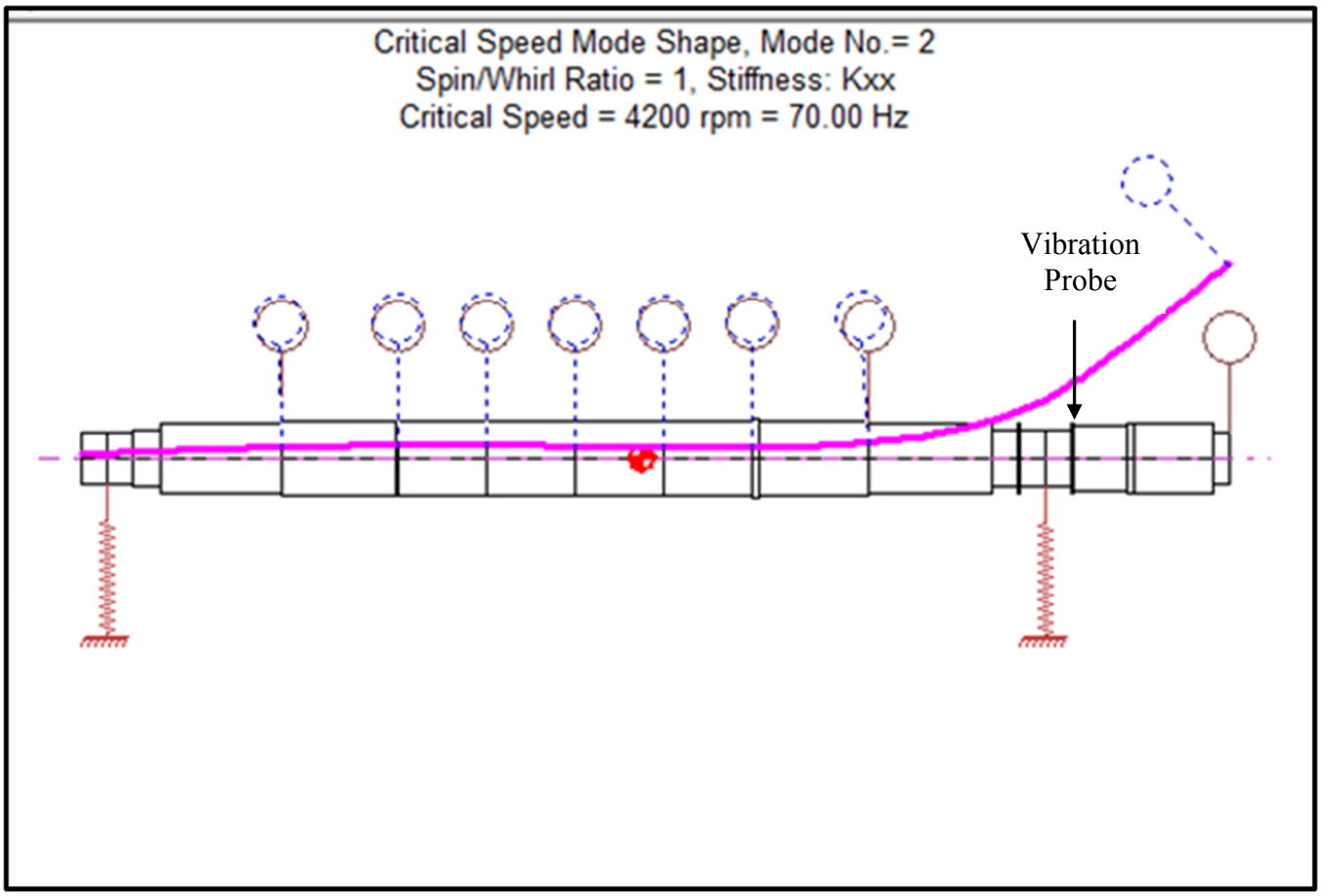

Figure 25: Case Study Three Motor Rotor Mode Shape

The unbalance response analysis with no coupling is shown in Figure 26. The following unbalances were used and these unbalances were all in phase with one another.

- DE fan: 3.4 oz-in (equivalent to 2W/N)
- Middle of Rotor Core: 6.8 oz-in (equivalent to 4W/N)
- NDE fan: 3.4 oz-in (equivalent to 2W/N)

As shown, there is a large response at about 1650 CPM, which corresponds with the first critical speed. There is virtually no response at the design operating speed of 2976 RPM at either the middle of the motor or at the DE bearing. The vibration probe is adjacent to the bearing on the DE side).

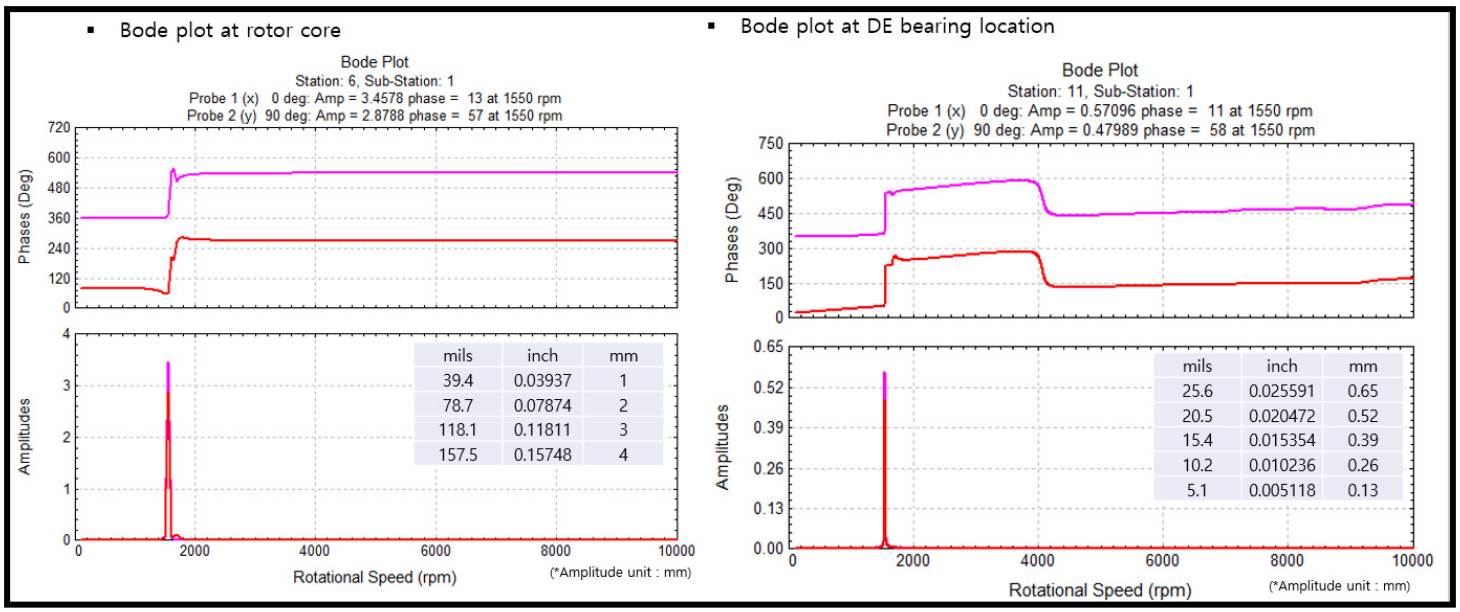

Figure 26: Case Study Three Unbalance Response – No Coupling

Then, the analysis was run again with the addition of the coupling. The coupling mass included the hub and 50% of the spacer/transmission unit. The following unbalances were used and these unbalances were all in phase with one another.

- Coupling: 6.8 oz-in (equivalent to 4W/N)
- DE fan: 3.4 oz-in (equivalent to 2W/N)
- Middle of Rotor Core: 6.8 oz-in (equivalent to 4W/N)
- NDE fan: 3.4 oz-in (equivalent to 2W/N)

The results are displayed in Figure 27. The response at the DE bearing, is a little higher at running speed, but does not explain the observed behavior in the field.

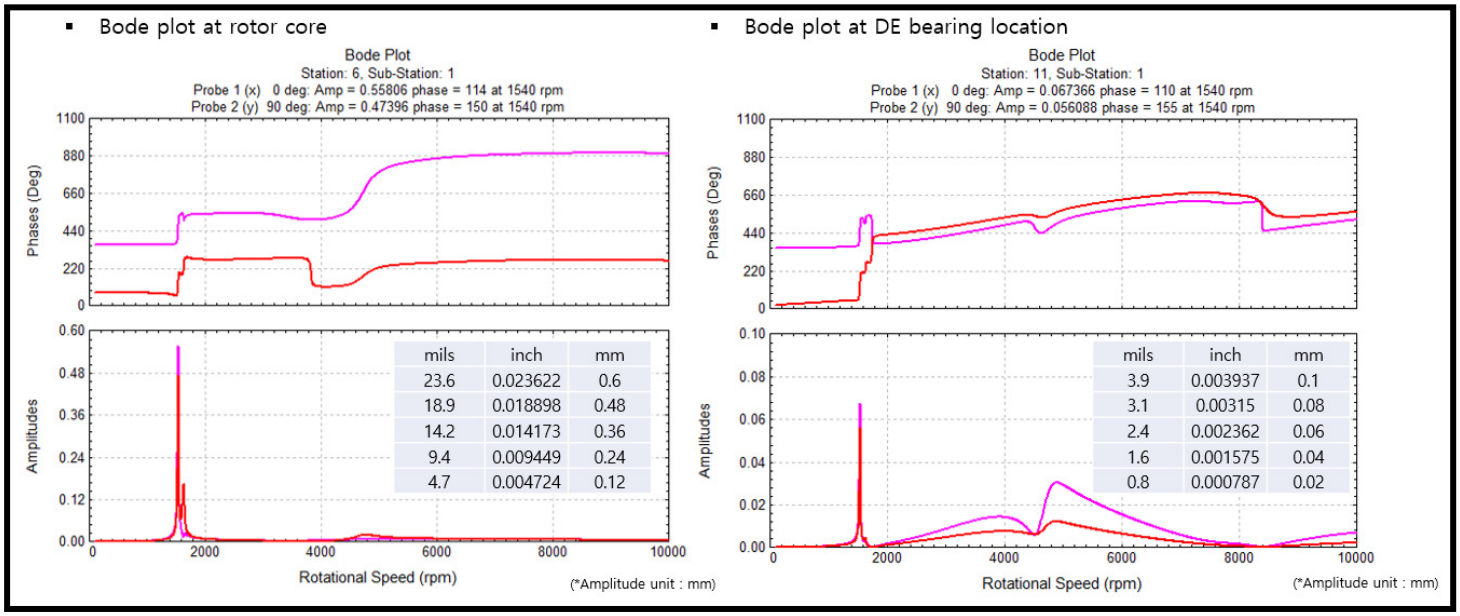

Figure 27: Case Study Three Unbalance Response With Coupling

Recall that during the field balance, 2.96 ounces (84 grams) of mass was added to the motor side coupling hub. Another analysis was then performed adding the equivalent amount of unbalance at the coupling (19.5 oz-in; equivalent to 11.5W/N). The results are displayed in Figure 28 and show a much larger response at the DE bearing at running speed.

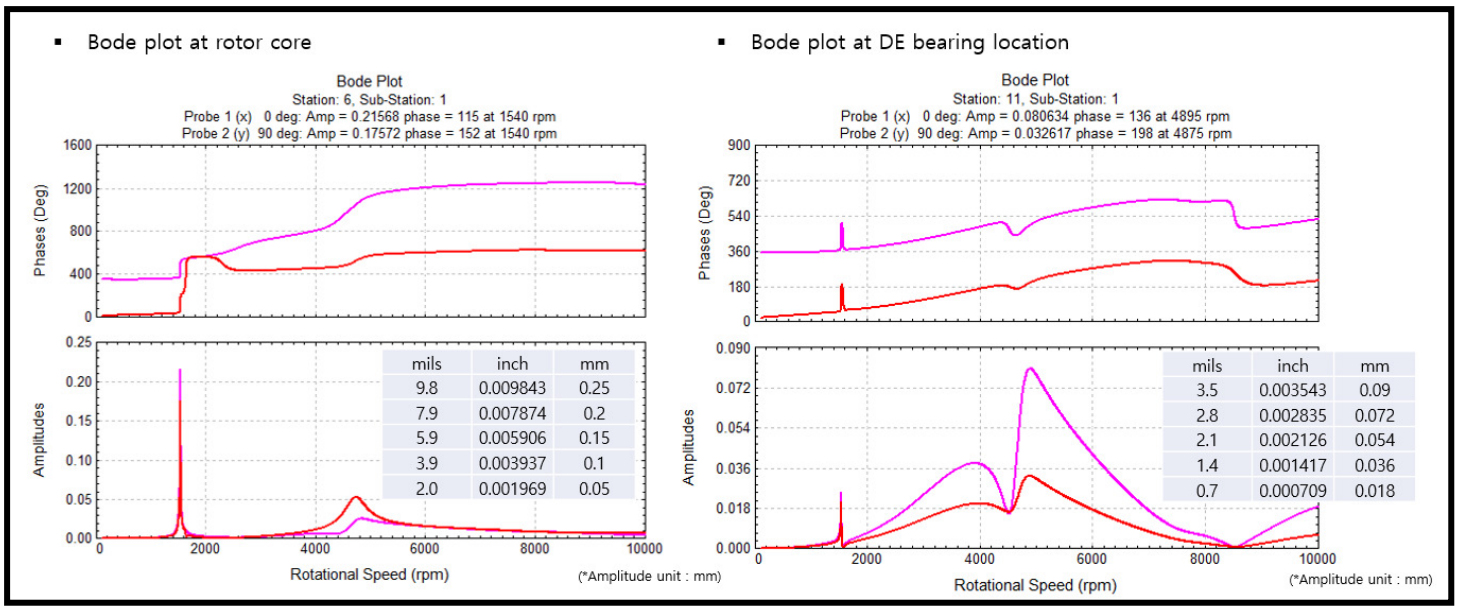

Figure 28: Unbalance Response With Coupling and 84 grams of Unbalance

Another analysis was performed, but this time the unbalance at the coupling was 180° out of phase with all the other unbalances. The results are displayed in Figure 29. As shown, there is a larger response at the middle of the rotor and the DE bearing at the critical speed. At running speed, the calculated response at the DE bearing was 1.0 mils p-p and was slightly higher than the analysis when all the unbalances were in phase with one another. These analyses show the sensitivity to unbalance distribution and phase relationship. Although the calculated response at the DE bearing did not equal what was observed in the field, the analyses did show that significant unbalance at the coupling was the likely cause.

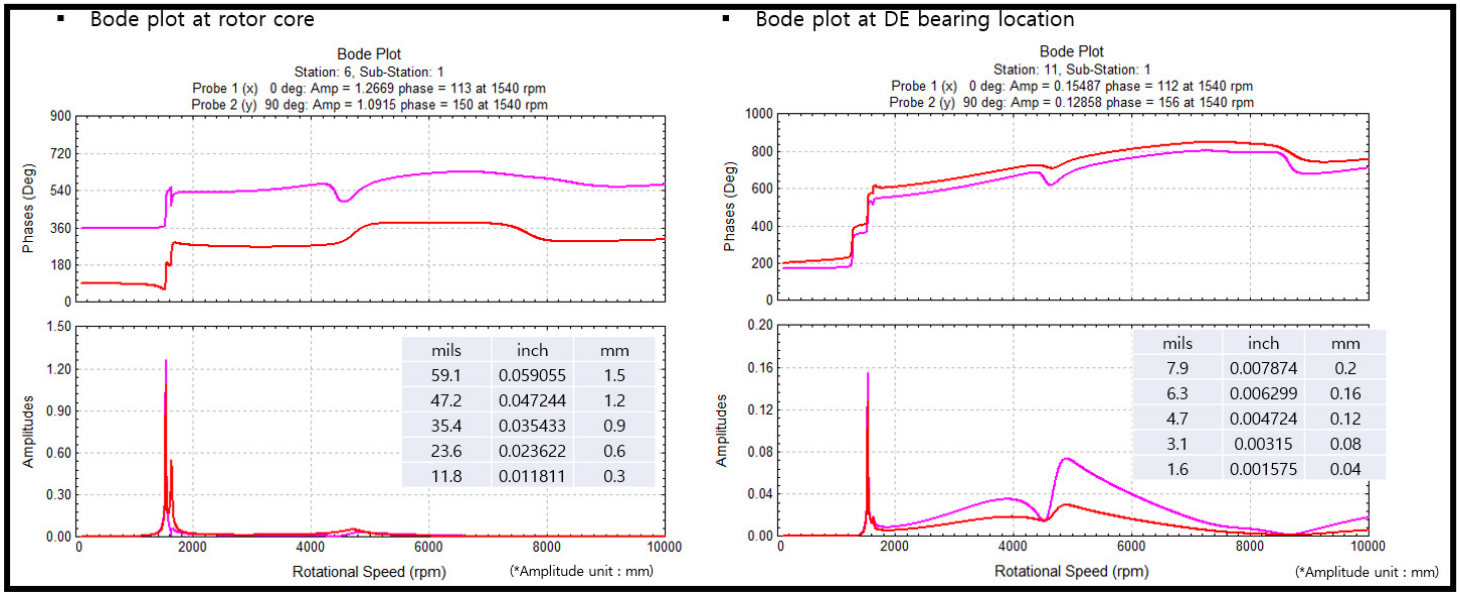

Figure 29: Case Study Three Unbalance Response With Coupling and DE Fan Unbalances 180° Out of Phase

The results of the rotordynamic analysis show how sensitive this rotor is to coupling unbalance, unbalance distribution and the unbalance phase relationship. Significant unbalance at the coupling is needed to explain the vibration behavior. But the coupling was well balanced and so what else could cause high unbalance? Runout checks were re-taken when the spare coupling was installed. A runout of 4 mils (.106 mm) was measured. This indicates an offset of 2.0 mils (.0508 mm). Using the mass of the motor half coupling hub and half the mass of the spacer/transmission unit, the calculated unbalance due to this mass offset results in an equivalent unbalance of 16.8 ounce-inches (12097 gram-mm), which is close to what was added in the field balance. So, it is likely that the problem was that the coupling was not concentric with the motor shaft.

CONCLUSIONS FOR CASE STUDY THREE

The motor lateral rotordynamics was not reviewed during the execution of the project. Although there was no issue with the rotordynamics, understanding the mode shape and unbalance response analysis provided a plausible explanation for the vibration behavior. The motor vibration when running without the coupling installed was acceptable. The vibration problems started as soon as the coupling hub was installed and got much worse when the full coupling was installed, especially with the original coupling. Performing a better coupling balance was clearly not the solution. There is no easy fix to this problem. Tighter control of the tolerances on the fits could help, but that would require new parts or significant rework. Although not ideal, the strategy is to field balance the coupled motor/compressor train whenever something is changed. And since the coupling change, the motor was replaced one time and the train was successfully field balanced.

When field balancing, it can be important to have an understanding of the rotordynamics. Motors that operate above the first lateral critical speed have some special challenges. Although the rotordynamics may be acceptable, the typical mode shape makes the rotor much more sensitive to overhung unbalance from the coupling and it is important to understand the phase relationship of the balance plane and the vibration measurement plane. And it is important to consider coupling balance criteria and concentricity tolerances of the coupling bore and fits.

CASE STUDY FOUR

Case study four pertains to a three stage integrally geared centrifugal compressor driven by a 4,962 HP, 1,783 induction motor. The gearbox consists of a bullgear and two rotors. The stage one/two rotor consists of a pinion with overhung impellers mounted each end. The stage three rotor consists of a pinion with a single overhung impeller on one end and a free end on the other side.

The gearbox utilizes tilting pad journal bearings for all three pinions with single non-contacting proximity type shaft vibration probes mounted in the air seal adjacent to each impeller. The pinions are fitted with thrust collars which transmit pinion axial thrust to the bullgear. The compressor configurate is shown in Figure 30.

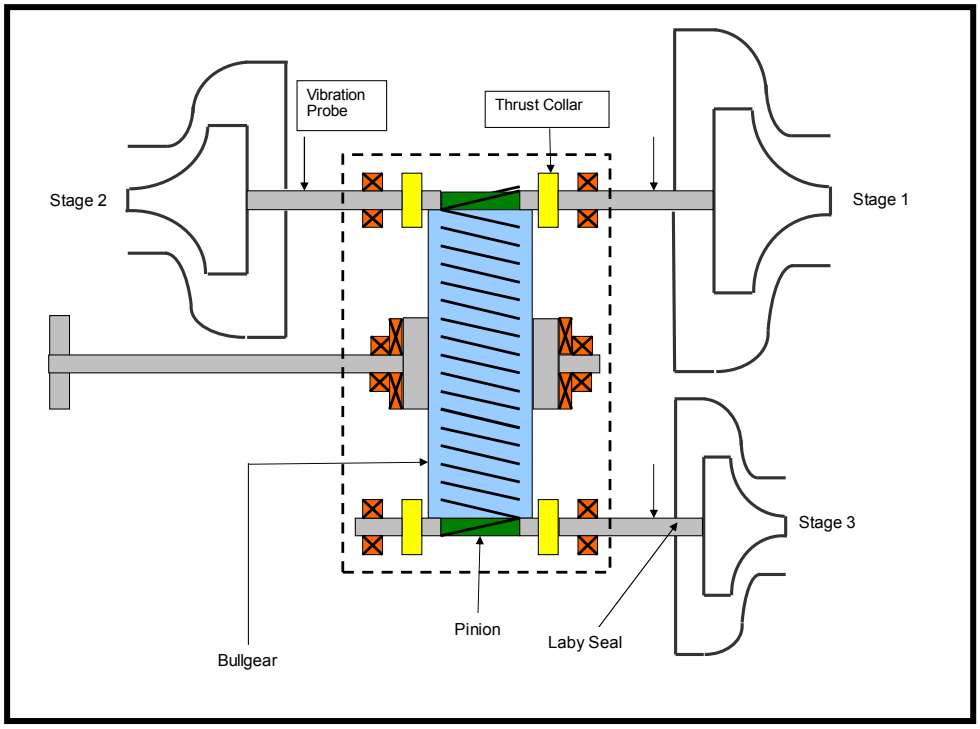

Figure 30: Case Study Four Compressor Configuration

The compressor supplier provided a lateral rotordynamic report as part of the project. When performing the damped unbalance analysis, the supplier did not use the 8W/N criteria discussed in API-684, but instead used an unbalance based on a given impeller Center-of Gravity displacement. The supplier stated in their experience, this is a more conservative approach for predicting the lateral rotordynamics of rotors with overhung impellers. Figure 31 shows the Bode plot for rotor one with these unbalances at both ends in phase with one another. The plot shows the predicted response at the second stage impeller. As shown, the predicted first critical speed is 9700 RPM and the amplification factor is 5.16. The rotor one operating speed is 14142 RPM, which works out to a separation margin of 39%, which complies with API-684.

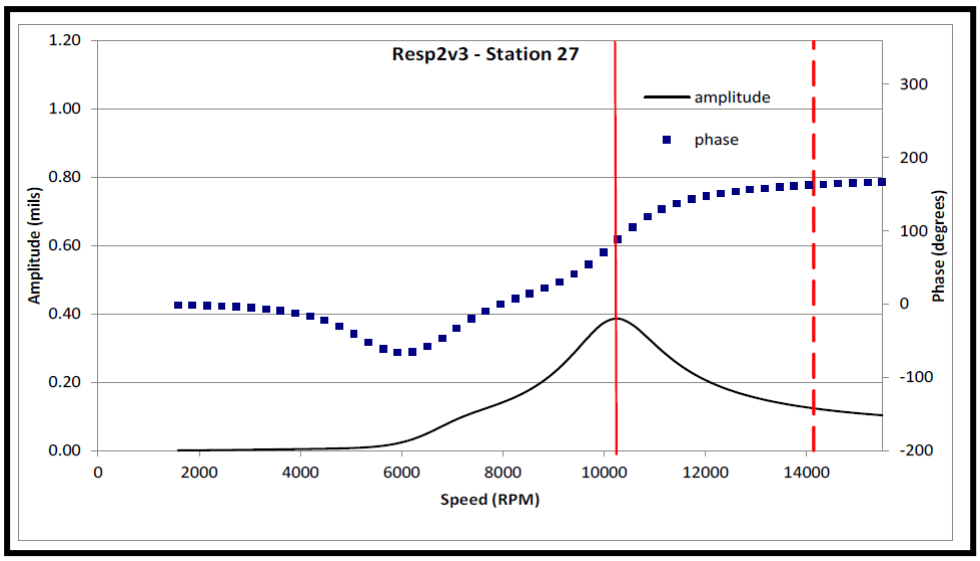

Figure 31: Case Study Four Second Stage Bode Plot

The compressor was mechanically tested in the supplier's shop. The compressor met the vibration acceptance criteria at the operating speed. However, there was a large response on coast down as the machine decelerated through the critical speed. There was some testing done at different oil pressures and the behavior changed, but it was still high and unexplained. See Figure 32. The vibration probe is located in the air seal near the back of the impeller, which is close to the location of the Bode plot that was done as part of the rotordynamic analysis. So, the shop test response at the critical speed was a surprise. As discussed in Case Study Three, the predicted behavior can be different because the actual unbalance and unbalance distribution is not as simple as what is done in the unbalance response analysis. However, this behavior was so significantly different that there was a concern of a possible mechanical issue. As a result, the shop test was rejected.

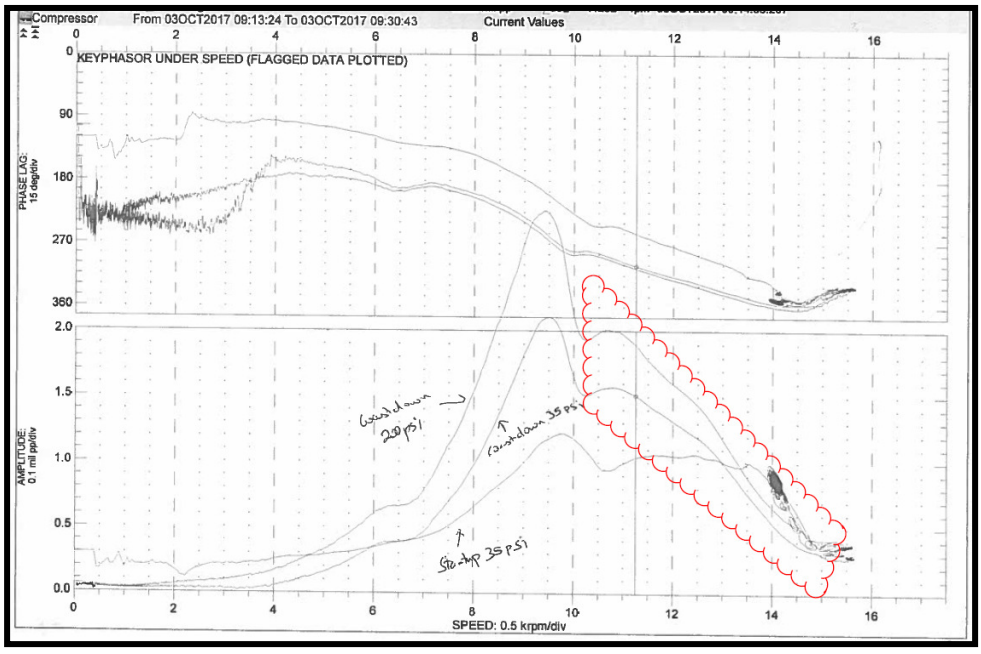

Figure 32: Case Study Four Initial Second Stage Coast Down Plot

The rotor was then removed and the second stage impeller unmounted. The impeller is hydraulically fit on the pinion shaft and there is a locating pin on the backside of the impeller. See Figure 33. The inspection revealed some rubbing contact between the pin and the locating hole in the pinion. This was unexpected and it was thought that this could cause a slight bending stress, which could exacerbate the vibration when the rotor passed through the critical speed. To correct this the locating hole was slightly enlarged and the rotor was reassembled and rebalanced. After retesting the vibration at the critical speed during coast down was greatly reduced. See Figure 34. In this figure, the red line is the coast down from the initial test and the blue line is the retest.

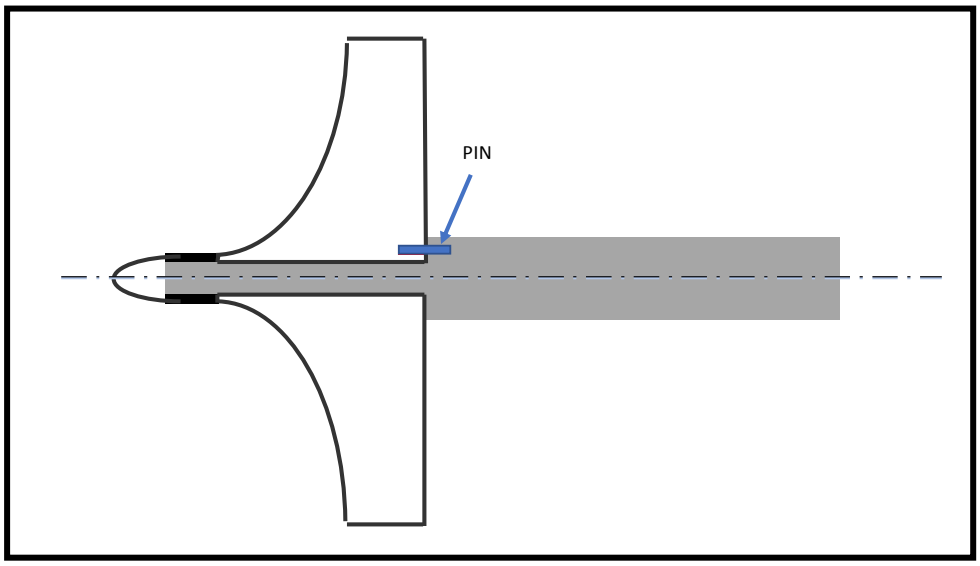

Figure 33: Case Study Four Second Stage Impeller Mounting

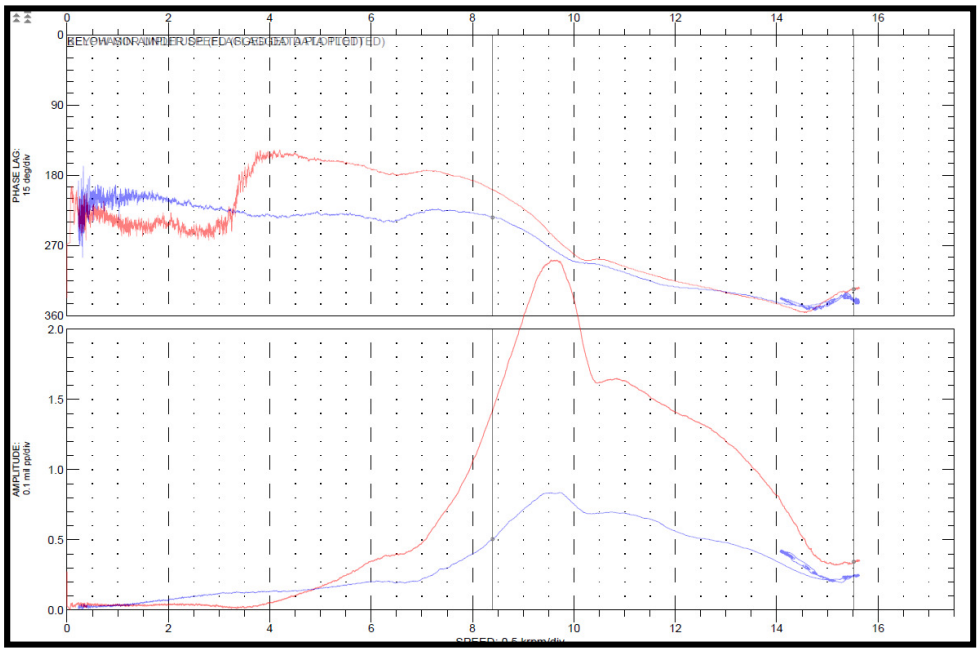

Figure 34: Case Study Four Stage Two Coast Down Plot

CONCLUSIONS FOR CASE STUDY FOUR

Whether the binding of the pin in the locating hole would cause future problems or not is not known. But it did have an impact on the coast down vibration of the second stage. This would not have been identified without reviewing the rotordynamics while evaluating the shop mechanical test results. Thus, reviewing the rotordynamics during the shop test can reveal potential problems which may have been missed without doing this.

CASE STUDY FIVE

Case study five pertains to a three stage inline centrifugal compressor driven by a steam turbine. The steam turbine is double acting with one side coupled to the inline compressor and the other side coupled to an integrally geared compressor. The inline compressor power at the design point is approximately 32 MW. The compressor design speed is 4190 RPM, with a maximum speed of 4400 RPM and a minimum speed of 4106 RPM. The compressor rotor consists of a shaft and three impellers. The first stage is overhung with an open impeller. Stages two and three are closed impellers and are mounted between the bearings. The rotor configuration is shown in Figure 35. Based on the rotordynamic analysis, the first three critical speeds are 2060 RPM, 2960 RPM and 5900 RPM.

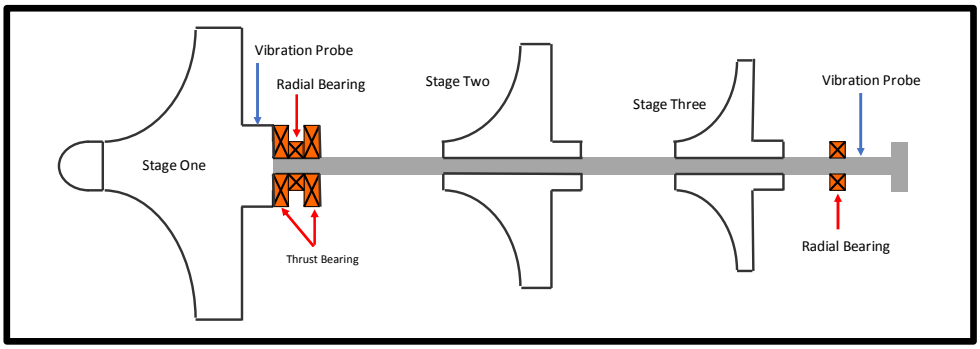

Figure 35: Case Study Five Rotor Bearing Arrangement

The vibration protection is active during start-up. The high vibration alarm set point was set at 2.8 mils p-p (70 microns) and the high vibration trip point was set at 3.5 mils p-p (90 microns). Although there is a vibration increase when accelerating through the first critical speed, based on the testing done during commissioning, the non-drive end (NDE) vibration peaked at 2.4 mils p-p (63 microns) and then dropped to about 0.9 mils p-p (24 microns) at the operating speed. So, no vibration trip multiplier was needed for start-up. This machine was started and stopped many times and about five months after commissioning, the machine tripped on high vibration during a start-up when attempting to accelerate through the first critical speed. A start-up vibration trip multiplier of 1.25X was added and the machine was successfully restarted. The NDE vibration at the first critical speed peaked at 3.9 mils p-p (98 microns) before dropping to 0.8 mils p-p (21 microns) at the operating speed. However, after several more starts the vibration multiplier had to be raised further to 1.5X, although the vibration at the operating speed remained unchanged. It was clear that the vibration when accelerating through the first critical speed was getting worse with every start and that this needed to be addressed. This is a large machine and it was important to identify and correct the problem on the first attempt to avoid opening the machine multiple times as this took a long time, took a lot of labor and required a large portable crane.

Based on the rotordynamic analysis, the first critical speed is an overhung mode at the NDE. The second critical speed is the first bending mode of the compressor shaft. In this mode, the deflection is highest between the bearings. The third critical speed is an overhung mode at the drive end (DE) and is above the operating speed. This mode shows little deflection at the overhung impeller at the NDE. As shown in Figure 35, the NDE vibration probe is located behind the impeller and intuitively, a balance issue with the stage one impeller could explain the behavior. The vibration going through the first critical would be high, but then would drop off and would not be affected as much at running speed. The balance issue could be due to impeller damage or loss of balance weights. There are balance weights on backside of the impeller.

The problem persisted to the point where the vibration was too high during start-up to ramp through the first critical speed. The machine was disassembled and the rotor was removed. A close inspection did not reveal any impeller damage or any missing balance weights (there was a record of the location and size of all the balance weights). The rotor was then sent to a 3rd party shop to do a high speed balance check. This shop had done high speed balancing of similar rotors for the compressor OEM in the past. Unfortunately, the vibration was so high when attempting to ramp through the first critical that the high speed balance had to be aborted. At this point it was clear there was a problem with the rotor.

The vibration data showed the vibration was clearly at one times (1X) operating speed, meaning it was all synchronous. And there did not appear to be a shift in the critical speed frequency. The runout was checked all along the rotor and there was two times the normal runout at the second stage impeller. The runout at the first and third stage impellers was okay. It appeared that there was a slight bend in the rotor at the second stage. Could this explain the behavior? The compressor manufacturer determined the bending stress needed to cause the equivalent runout to what was measured and then applied this in a rotordynamic analysis. The analysis matched the observed behavior at the first critical speed, which showed that the vibration at the NDE was about twice the vibration at the DE end. The compressor manufacturer did another analysis applying an unbalance in middle of the rotor and at first stage to get a similar bend in the rotor based on the measured runout. The analysis showed similar results with adding the bending moment at second stage impeller. This showed that the analysis is less dependent on unbalance distribution with the bent rotor. The decision was made to de-stack the rotor. In the process of heating the second stage impeller for destacking, the rotor straightened. After removing all the impellers, fretting damage was discovered on the shaft at the nose of the 2nd stage impeller. There is a light shrink fit at the nose of the impeller. During operation at some speeds this can lose contact with the shaft. The torque is carried by the shrink at the back of the impeller. The lift off speed was within the operating speed range of the compressor. It was concluded that it is was likely the bore under the nose of the impeller was rubbing against the shaft during operation and on start-up and shutdown. And, once the damage was sufficient, the impeller nose would grab the shaft and bend it. On start-up the vibrations would be elevated until the nose lifted off and the shaft would straighten. To address this, the shaft was slightly undercut under the nose of the second stage impeller. This area does not carry any torque at full speed. See Figure 35.

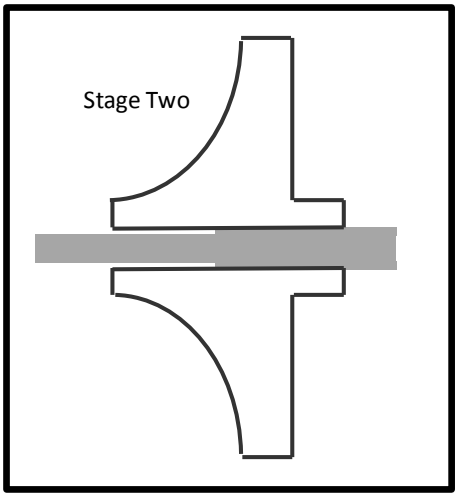

Figure 35: Case Study Five Showing Exaggerated Undercut at Impeller Nose

After this correction was implemented, no other problems have occurred.

CONCLUSIONS FOR CASE STUDY FIVE
This was not an easy problem to diagnose. Removing the rotor was considerable work as was destacking the rotor. It also had a significant impact on the customer. So, when making corrections, it was important to have as much confidence as possible in identifying the problem and coming up with a solution. Understanding the rotordynamics and doing additional analyses to support the root cause analysis went a long was in doing this.

CONCLUSIONS
As shown in this tutorial and the case studies, understanding rotordynamic analysis can be very helpful in identifying and solving vibration problems in turbomachinery. There are times when outside help may still be needed, but end users can still benefit by being able to participate in the root cause analysis, suggest possible solution and evaluate the risks. End users don't need to be experts in performing the rotordynamics, but understanding the information and results allows end users to make better decisions.

Variables
F = Force
m = Mass
a = Acceleration
k = Spring stiffness
x = Displacement
t = Time
ω = Undamped natural frequency
ω_d = Damped natural frequency
C = Coefficient of viscous damping
υ = Velocity
Ccrit = Critical damping coefficient
ζ = Damping ratio
δ = Log dec
β_d = Damped magnification factor
ω_f = Forcing function frequency

REFERENCES
API-612, 2014, "Petroleum, Petrochemical, and Natural Gas Industries—Steam Turbines—Special-purpose Applications," Seventh Edition, American Petroleum Institute. Washington, DC.

API-617, 2016, "Axial and Centrifugal Compressors and Expander-compressors for Petroleum, Chemical and Gas Industry Services,"

Eighth Edition with Errata, American Petroleum Institute. Washington, DC.

API-672, 2010, "Packaged, Integrally Geared Centrifugal Air Compressors for Petroleum, Chemical, and Gas Industry Services," Fourth Edition with Errata, American Petroleum Institute. Washington, DC.

API-684-1, 2019, "API Standard Paragraphs Rotordynamic Tutorial: Lateral Critical Speeds, Unbalance Response, Stability, Train Torsionals, and Rotor Balancing," First Edition, American Petroleum Institute. Washington, DC.

Pavelek, D. and Kelm, R., 2020, "Turbomachinery Rotordynamics: Modeling, Analysis and Reporting Overview", AIChE Paper 37e, AIChE Spring Meeting and Global Congress on Process Safety.

Smith, P. Whalen, J., Benton, R., Obeid, V. "Methods to Effectively Evaluate Modern Journal Performance and Achieve high Reliability," *Proceedings of the Forty Eighth Turbomachinery Symposium*, Turbomachinery Laboratory, Texas A&M University, College Station, Texas, 2019. https://hdl.handle.net/1969.1/188631

Smith, Patrick J., "Squeeze Film Dampers for Turbomachinery," Energy-Tech Magazine, May 2010

Whalen, J., Hess, T., Allen, J., Craighton, J., "Babbitted Bearing Health Assessment", *Proceedings of the Forty First Turbomachinery Symposium*, Turbomachinery Laboratory, Texas A&M University, College Station, Texas, 2012. https://doi.org/10.21423/R1135H

Nicholas, John C.; Whalen, John K.; Franklin, Sean D., "Improving Critical Speed Calculations Using Flexible Bearing Support FRF Compliance Data", *Proceedings of the Fifteenth Turbomachinery Symposium*, Turbomachinery Laboratory, Texas A&M University, College Station, Texas, 1986. https://doi.org/10.21423/R1B09S

Lindenburg, Michael R., Mechanical Engineering Reference Manual for the PE Exam, 11th Edition, Professional Publications, Inc., Belmont, CA, 2001

ACKNOWLEDGEMENTS